Role of Nup93 subcomplex in HOXA gene regulation during NT2/D1 differentiation

A thesis

submitted to

Indian Institute of Science Education and Research Pune

in partial fulfilment of the requirements for the

BS-MS Dual Degree Programme

by

Adwait Bhalchandra Salvi

Indian Institute of Science Education and Research Pune

Dr. Homi Bhabha Road,

Pashan, Pune 411008, INDIA.

April 2019

Supervisor: Kundan Sengupta

Certificate

This is to certify that this dissertation entitled “Role of Nup93 subcomplex in HOXA gene regulation during NT2/D1 differentiation” towards the partial fulfillment of the BS-MS dual degree programme at the Indian Institute of Science Education and Research (IISER) Pune, represents original research carried out by Adwait Bhalchandra Salvi at CHROMOSOME BIOLOGY LAB (CBL), IISER Pune under the supervision of Dr. Kundan Sengupta, Associate Professor, IISER Pune during the academic year 2018-2019.

Kundan Sengupta
Associate professor, Dept. of Biology,
IISER, Pune
31.3.2019

Declaration

I hereby declare that all the matter embodied in the report entitled “Role of Nup93 subcomplex in HOXA gene regulation during NT2/D1 differentiation” are the results of the investigations carried out by me at the Department of Biology, Indian Institute of Science Education and Research (IISER) Pune, under the supervision of Dr. Kundan Sengupta, Associate Professor, IISER Pune and the same has not been submitted anywhere else for any other degree.

Adwait Salvi
20141088
BS-MS
IISER, Pune
31.3.2019

Abstract

Nuclear Pore complexes (NPCs) are multiprotein complexes embedded in the nuclear envelope that facilitate the regulated transport of RNA and proteins between nucleus and cytoplasm. NPCs consist of ~30 different types of nucleoporins. Recent evidences suggest an involvement of nucleoporins in regulation of gene expression and cell differentiation. Here we investigated the role of Nup93 subcomplex in the regulation of HOXA gene expression during differentiation of NTera2.D1 embryonal carcinoma cell line, which differentiates into a neuronal lineage in response to retinoic acid (RA). We show that Nup93 and CTCF antagonistically regulate HOXA gene expression. Nup93 shows an altered occupancy on HOXA gene promoters during differentiation. We also report for the first time the four copies of HOXA gene cluster are repositioned proximal to the nuclear periphery during RA mediated differentiation in the interphase nucleus. We have shown that the interactors of Nup93 subcomplex independently regulate HOXA gene expression. Taken together our data uncovers a novel role for Nup93 and CTCF in modulating the spatiotemporal localization and function of the HOXA gene locus during differentiation.

Index

List of Figures and Tables:

Acknowledgement

I convey my sincere gratitude to Dr. Kundan Sengupta, Chromosome Biology Lab, Indian Institute of Science Education and Research, Pune, for allowing me to work in his lab and his valuable guidance during this project. I also thank him for his support in pursuing my ideas. I am grateful to Dr. Ajay Labade for his constant support and for guidance throughout the project. This project would not have succeeded without his immense help. I would like to thank all CBL lab members for their guidance and critical peer review, which helped me refine my ideas.

I express my gratitude towards Dr. Sanjeev Galande and Dr. Rini Shah, IISER-Pune for their help and guidance. I also thank Dr. Peter Andrews, University of Sheffield, USA and Dr. Jomon Joseph, NCCS Pune. I thank IISER Pune for providing me with excellent infrastructures and opportunities over last five years.

Introduction

Nuclear Pore Complexes (NPCs) are one of the largest macromolecular assemblies in cells. These complexes enable regulated transport of molecules across the nuclear envelope. NPCs range from 90-150 MDa and show 8 fold symmetry. NPCs have four components – cytoplasmic filaments, transmembrane scaffold, nuclear ring and nuclear basket. NPCs consist of ~30 different nups or subunits which together facilitate transport (Raices and D'Angelo 2012). NPCs also function as a landmark for gene regulation (Pascual-Garcia and Capelson 2014). Along with the well-studied role of Nups in nuclear transport, recent studies have highlighted the involvement of nups in gene regulation as well as differentiation. Nup210 interacts with Mef2C and regulates muscle development in zebrafish (Raices et al. 2017). Nup98 interacts with trx/MLL complex and regulates gene expression through chromatin loops (Pascual-Garcia et al. 2014). Nup93 Dam-ID experiment revealed genome wide binding of Nup93. Nup93 binds to super-enhancers (clusters of enhancers) and regulates expression of cell identity genes (Ibarra et al. 2016). Nup93 is a scaffold nucleoporin which is stably present at the NPC (Fig.1). Even though the structure of the mammalian nuclear pore complex subunits and Nup93 is not resolved, structure of its yeast homolog (Nic96) has been elucidated (Jeudy and Schwartz 2007). Mammalian Nup93 contains Nic96 domain and additional ~200 amino acids at N terminal. Nup93 subcomplex is present in 32 copies in transmembrane scaffold of NPC. Nup93 and its immediate interactors Nup188 and Nup205 have very high stability. In a pulse chase experiment, pregnant female mice were fed with radioactive isotopes and 6 months after birth, cells from pups were examined for proteins containing these isotopes. It was found that several proteins including Nup93, Nup188 and Nup205 showed only ~50% turnover in 6 months (Toyama et al. 2013). Such stability and peripheral localization suggests Nup93 as an important gene regulator. Nup93 potentially tethers and represses HOXA gene expression. HOXA repression is facilitated by Nup188 and Nup205. Nup93 associates with the promoters of HOXA1, HOXA3 and HOXA5 genes respectively (Labade et al. 2016). Nup93 ChIP-seq suggests its association with genes involved in development (unpublished data). Interestingly, CTCF motif was enriched in Nup93 binding sites. CTCF (CCCTC binding protein) is a genome organizer and regulates genome

organization through chromatin looping. CTCF peaks were found to overlap with Nup93 peaks genome wide (unpublished data). These observations suggest a potential overlap of Nup93 and CTCF in regulating HOXA cluster.

Here we investigated the role of Nup93 and CTCF in regulating the spatiotemporal dynamics of HOXA organization and function in a model of cell differentiation. We selected NTera2.D1 embryonal carcinoma cells derived from human teratocarcinoma as a model, since it differentiates into the neuronal lineage in response to Retinoic Acid (RA) treatment (Xu et al. 2014).

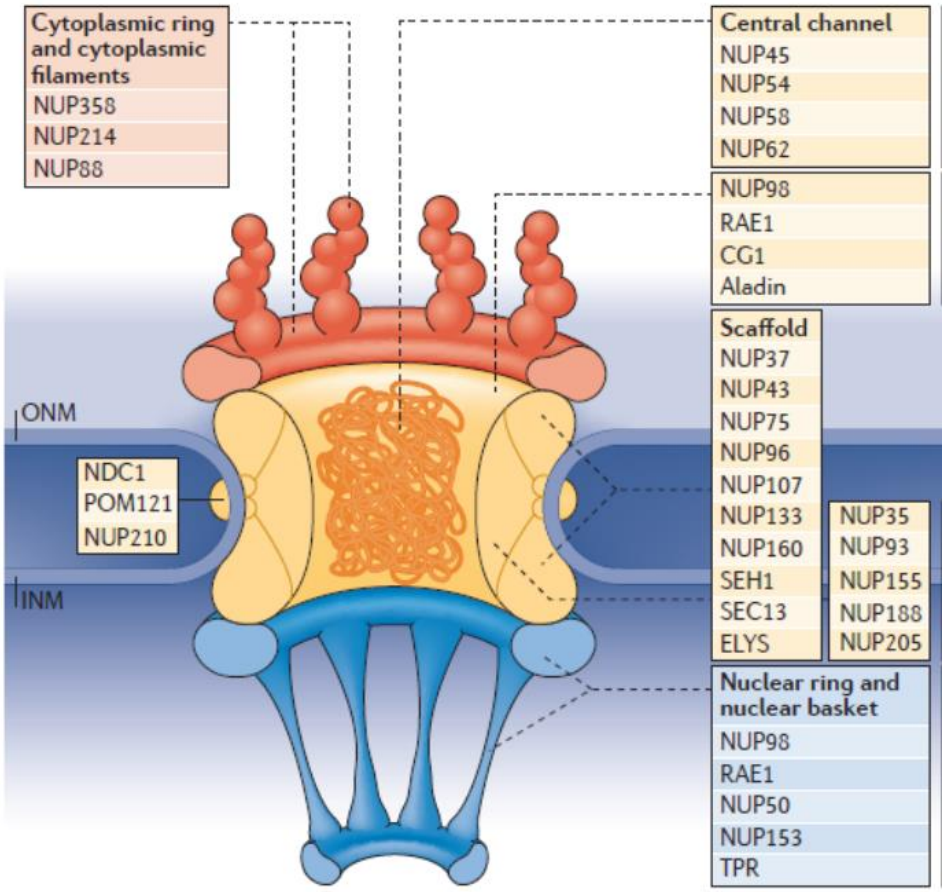

Fig1: Structure of mammalian nuclear pore complex. *Image adapted from (Raices and D'Angelo 2012)*

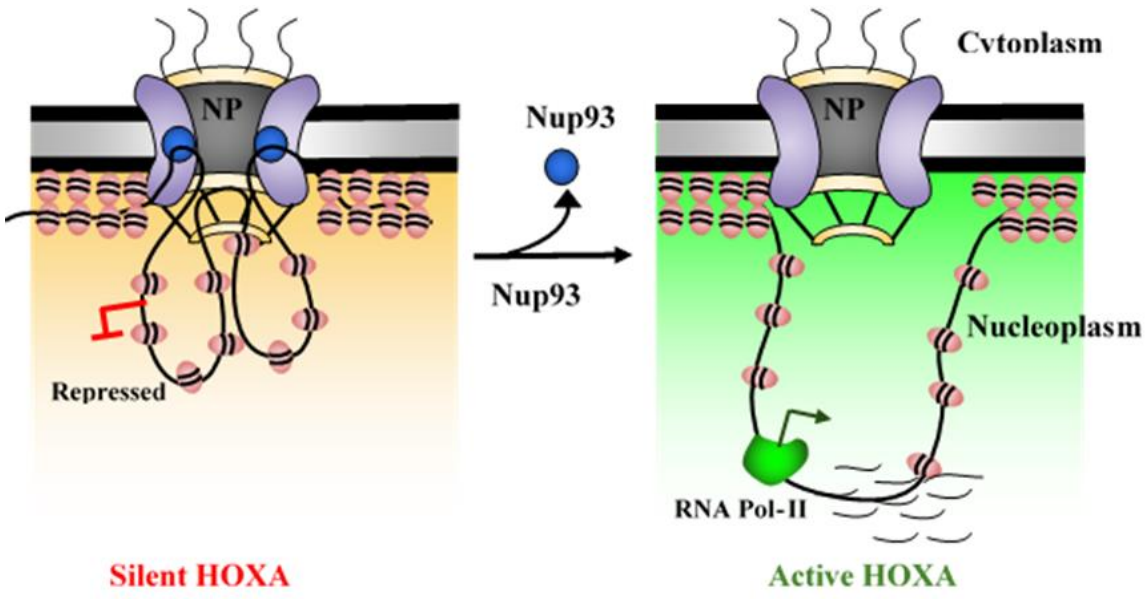

Fig2: Nup93 represses HOXA gene cluster by functioning as a stable tether at the nuclear periphery. *Loss of Nup93 upregulates HOXA expression as HOXA gene locus moves away from the nuclear periphery. Adapted from Labade, Ajay, 2018, (Doctoral thesis) 'The role of nucleoporin Nup93 subcomplex in regulating HOXA gene expression' Chromosome Biology Lab, IISER-Pune*

Teratocarcinomas are a subset of germ cell tumors and are highly malignant. Teratocarcinomas harbor many somatic as well as extraembryonic cell populations along with pluripotent cells. These undifferentiated tissues in teratomas often resemble embryonal tissues and hence are termed as embryonal carcinoma (EC) (Andrews et al. 2005). EC cell lines - P19 (mouse) and NT2/D1 (human) proliferate in vitro (Kelly and Gatie 2017). EC cells differentiate when treated with appropriate stimulus (e.g. retinoic acid). NTera2.D1 cells can be cultured while retaining their potential to differentiate. This differentiation paradigm resembles Embryonic Stem cells (ES cells), which are derived from the inner cell mass of blastocysts. EC cells present an alternative paradigm to study cell differentiation. NT2/D1 cells differentiate irreversibly to the neuronal lineage in response to Retinoic Acid and are therefore considered precursors of human neuronal cells. Similarly, NT2/D1 cells also differentiate into epithelial lineage upon treatment with Bone Morphogenic Protein (BMP) (Caricasole et al. 2000). These studies together highlight that NT2/D1 cells function as a robust model for studying differentiation.

Addition of Retinoic Acid (RA) to NT2/D1 cells, upregulates HOX gene expression (Xu et al. 2014). Homeobox gene clusters control differentiation and patterning during development. Since their discovery in patterning over 3 decades ago in *Drosophila*, many studies have underlined the role of HOX genes in development (Mallo et al. 2010). HOX genes exhibit collinear expression i.e. linearity in expression which resembles their physical location on the chromosome. Through evolution, HOX genes in *Drosophila* have diversified and formed 4 different clusters (HOXA, HOXB, HOXC and HOXD) in mammals (Mallo et al. 2010). Even though the effect of HOX genes in development is known; precise mechanisms regulating temporality of HOX expression are still obscure. Since RA treatment increases HOX gene expression across all 4 four clusters, NT2/D1 cells are a useful system to study the temporal expression of HOXA. A recent study by Xu et al highlighted the role of CTCF in regulating HOXA gene expression during RA mediated differentiation (Xu et al. 2014). This study suggests that CTCF regulates 3D organization of the HOXA gene cluster during differentiation and assists in HOXA expression during the early phase of differentiation (Day 4). The study also showed that upregulation of 3' HOXA genes declines by Day 8 (Xu et al. 2014).

We first characterized the differentiation potential of NT2/D1 cells across an 8-day time regimen. Expression levels of HOXA genes upon treatment with RA were quantified. Also levels of Nup93, Nup93 interactors, pluripotency markers (Oct4, Sox2 and Nanog), and CTCF were examined during the 8 day differentiation period. Pax6 expression was examined to ascertain that NT2/D1 cells indeed differentiate into a neuronal lineage (Zhang et al. 2010). We performed Fluorescent in Situ Hybridization (FISH) to examine the dynamics of the HOXA gene locus during differentiation. We also studied features of nuclear topology such as volume, surface area and sphericity during cell differentiation. To uncover how Nup93, Nup188 and Nup205 contribute to HOXA gene regulation during differentiation, expression levels of HOXA genes upon transient knockdown of these nups in presence as well as absence of RA were quantified. Binding of Nup93 and CTCF on sites within HOXA cluster was determined using Chromatin Immunoprecipitation. In summary, this study uncovers interesting facets of the dynamics of the HOXA gene cluster during differentiation.

Results

Characterization of NT2/D1 cell differentiation

NT2/D1 cells differentiate into the neuronal lineage when treated with Retinoic acid (RA). We observed characteristic morphological changes in cells upon RA treatment (Fig. 3A). Cells typically become elongated and flat, suggestive of neuronal differentiation upon RA treatment. As a marker of differentiation - Oct4, Sox2 and Nanog expression was examined. While Oct4 expression levels showed a marginal decrease on Day 2, this declined rapidly with time, indicative of differentiation upon RA treatment (Fig. 3B). Sox2 showed a similar pattern of expression (Fig. 3C). Nanog expression however, decreased rapidly from Day 2 onwards (Fig. 3D). Pax6 expression showed moderate increase till Day 2, followed by a massive increase on Day 4 (~250 fold) and decrease on Day 8 (~100 fold) (Fig. 3E). Overall increase in Pax6 expression suggests that NT2/D1 cells potentially differentiate into the neuronal lineage. Oct4 levels were examined using western blotting (Fig. 1F). Similar to Oct4 expression, Oct4 levels decreased significantly on Day 4 and Day 8 (Fig. 1G). Also Oct4 levels determined by IFA showed high levels on Day 0 but no detectable Oct4 was seen on Day 4 and Day 8 (Fig. 1H).

HOXA gene expression during RA treatment

HOXA genes are upregulated during NT2/D1 differentiation. HOXA gene expression was tested in RA treated NT2/D1 cells using RT-qPCR. HOXA1 gene present at 3' end (Fig. 4A) of HOXA gene cluster was upregulated early, attained maximum levels of expression by Day 2 (~200 fold), followed by a gradual decline on Day 4 and 8 (Fig. 4A,B). In accordance with the collinearity of the HOXA gene cluster - HOXA5 and HOXA9 genes were upregulated toward the late phase (Day 4-8). HOXA5 and HOXA9 expression increased with time and was maximally upregulated on Day 8 (~2500 fold) (Fig. 4C,D). HOXA13 (5' end) expression was low as compared to other HOXA genes, but increased gradually with time and peaked on Day 8 with ~5 fold upregulation (Fig. 4E). Expression levels of HOXA1, HOXA5, HOXA9 and HOXA13 on Day 2 underscores the collinearity and temporality of HOXA gene expression with 3' genes in the cluster showing overexpression as compared to the 5' genes (Fig. 4F).

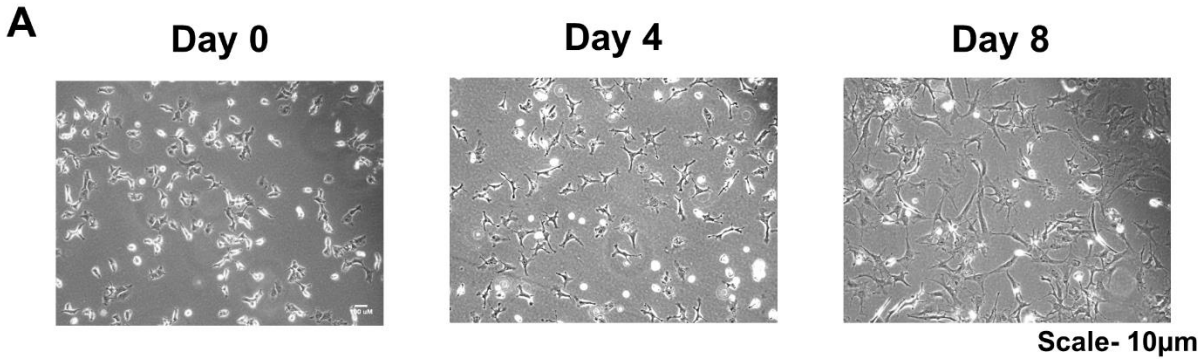
A
Day 0
Day 4
Day 8
Scale- 10µm

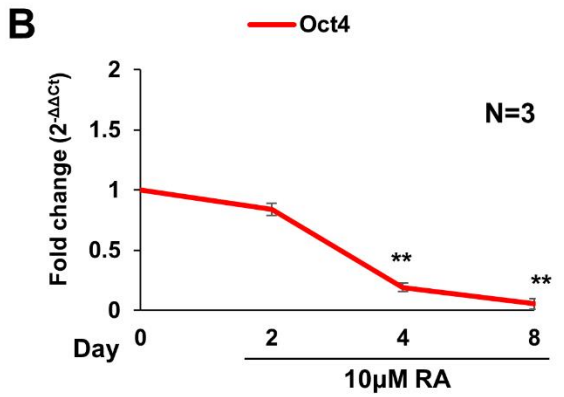
B
Oct4
Fold change (2-ΔΔCt)
N=3
Day
10µM RA

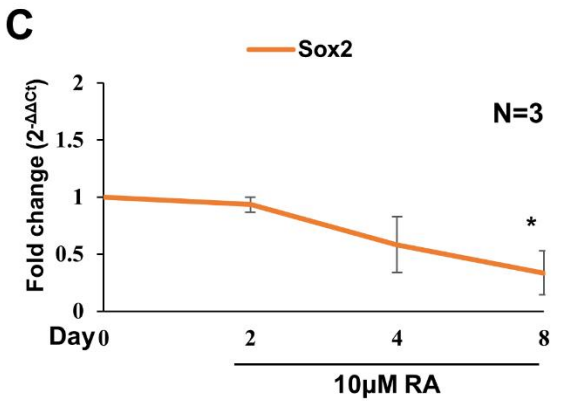
C
Sox2
Fold change (2-ΔΔCt)
N=3
Day
10µM RA

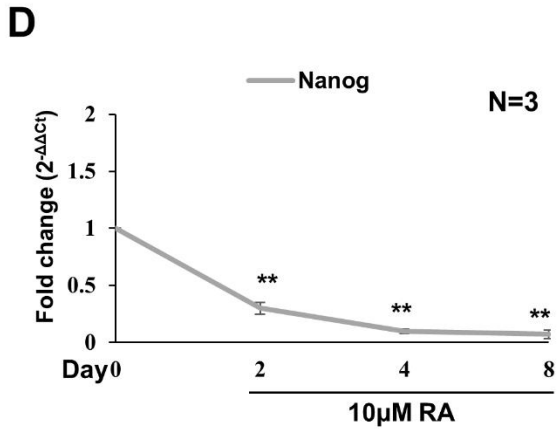
D
Nanog
Fold change (2-ΔΔCt)
N=3
Day
10µM RA

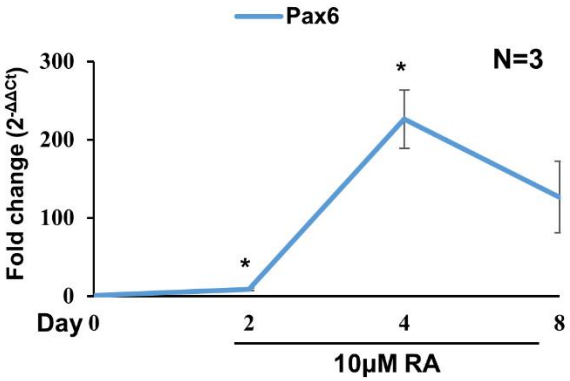
E
Pax6
Fold change (2-ΔΔCt)
N=3
Day
10µM RA

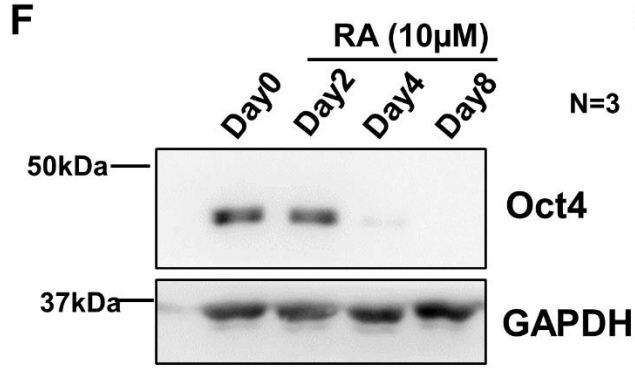
F
RA (10µM)
Day0
Day2
Day4
Day8
N=3
50kDa
Oct4
37kDa
GAPDH

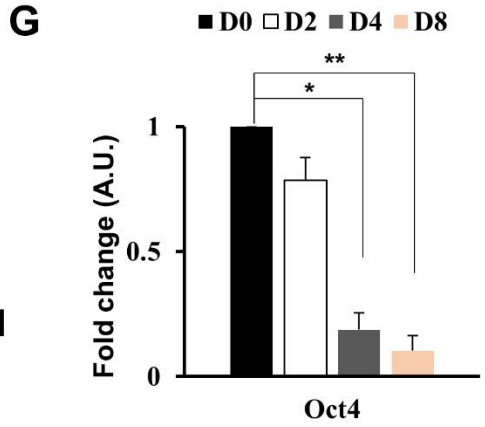
G
D0 D2 D4 D8
Fold change (A.U.)
Oct4

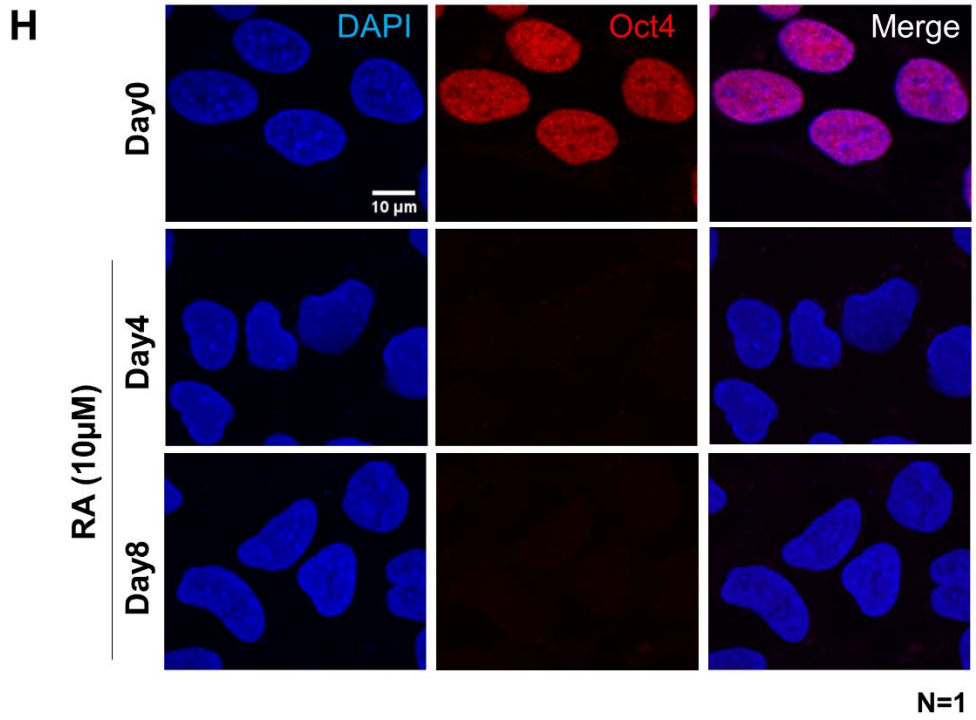

Fig 3: Characterization of NT2/D1 differentiation. *(A) Morphological changes in cells upon RA treatment (B) Oct4 (C) Sox2 (D) Nanog and (E) Pax6 expression levels on Day 0,2,4 & 8. Data from 3 biological replicates. Error bars represent SEM. Significance calculated using t test. (* = p<0.05, ** = p<0.01) (F) Oct4 levels on Day 0,2,4 & 8. (G) Quantification of (F). Data from 3 biological replicates. (* = p<0.05, ** = p<0.01) (H) Oct4 staining on Day0, 4 & 8. Scale bar = 10µm.*

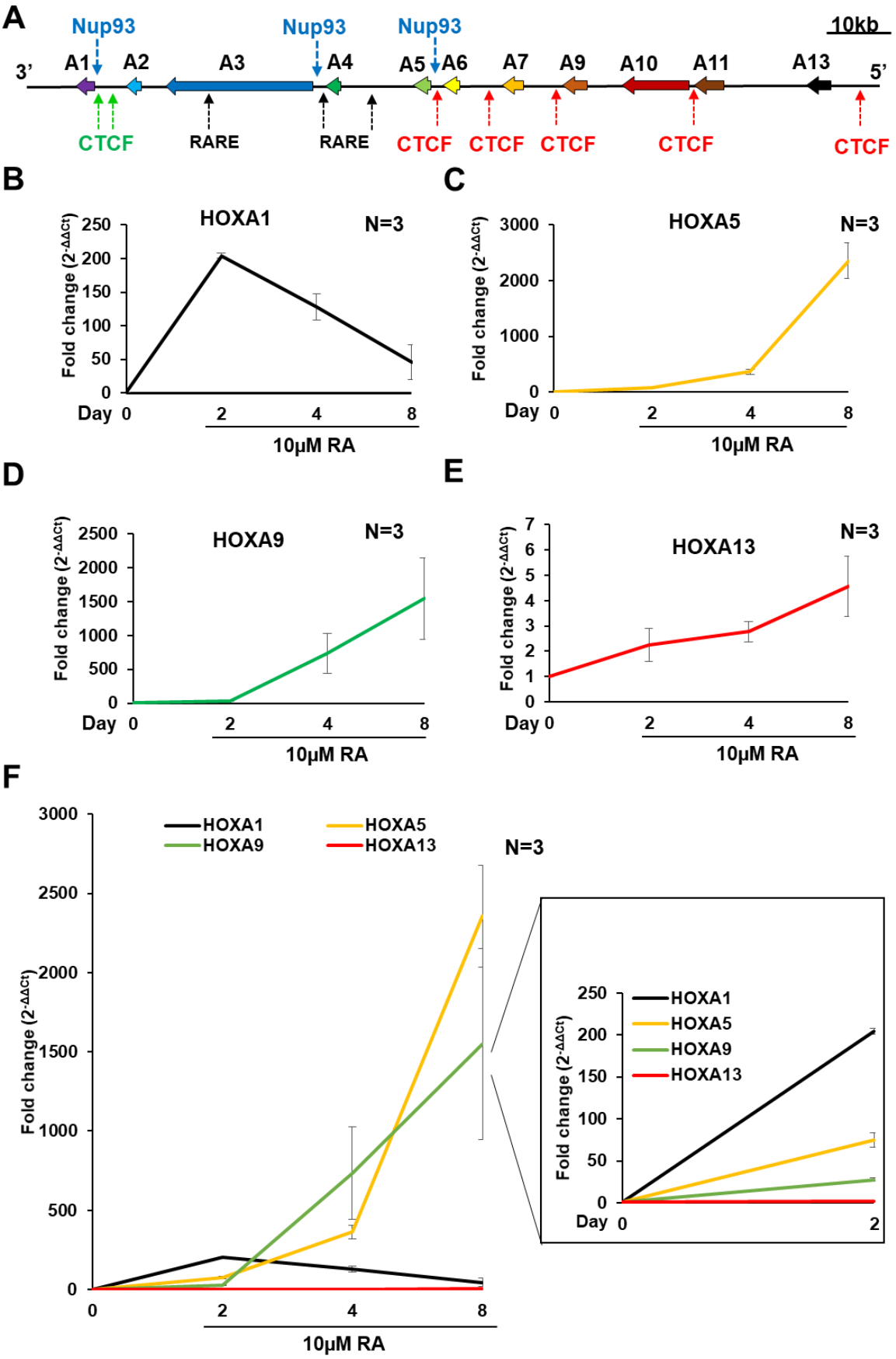
A
Nup93
Nup93
Nup93
10kb
3'
A1
A2
A3
A4
A5
A6
A7
A9
A10
A11
A13
5'
CTCF
RARE
RARE
CTCF
CTCF
CTCF
CTCF
CTCF
B
HOXA1
N=3
Fold change (2-ΔΔCt)
Day
10μM RA
C
HOXA5
N=3
D
HOXA9
N=3
E
HOXA13
N=3
F
HOXA1
HOXA5
HOXA9
HOXA13
N=3

Fig4: HOXA gene expression during NT2/D1 differentiation *(A) Schematic of HOXA cluster showing Nup93 (blue arrows), conserved CTCF (red arrows), non-conserved CTCF (green arrows) binding sites and RARE elements (black arrows). HOXA1 (B), HOXA5 (C), HOXA9 (D), HOXA13 (F) expression levels on Day 0,2,4,8. (E) Combined expression data from B-E. Data from three biological replicates. Error bars represent SEM.*

Localization of HOXA gene locus during cell differentiation

It is well established that heterochromatin which is typically proximal to the nuclear envelope is a largely a repressive environment (Buchwalter et al. 2019). Furthermore, movement of genes (such as Nid1, Ptn, and Cxcl1) away from nuclear periphery correlates with their transcriptional activation (Robson et al. 2016), we therefore examined the localization of HOXA gene locus during differentiation, using Fluorescent In Situ Hybridization (FISH) (Fig. 5A). We measured the shortest distance of the HOXA gene locus with respect to the nuclear periphery across Day 2 to Day 8 upon RA treatment. NT2/D1 cells are aneuploid and have 4 copies of the HOXA gene locus. Interestingly, the distance of the HOXA gene cluster from the nuclear periphery, increased on Day 2 (median = 1.61µm) and Day 4 (1.5µm), as compared to Day 0 (1.12µm) (Fig. 5B). However, on Day 8, median distance decreased (1.18µm), suggesting a movement of the HOXA gene loci back to nuclear periphery (Fig. 5B,C).

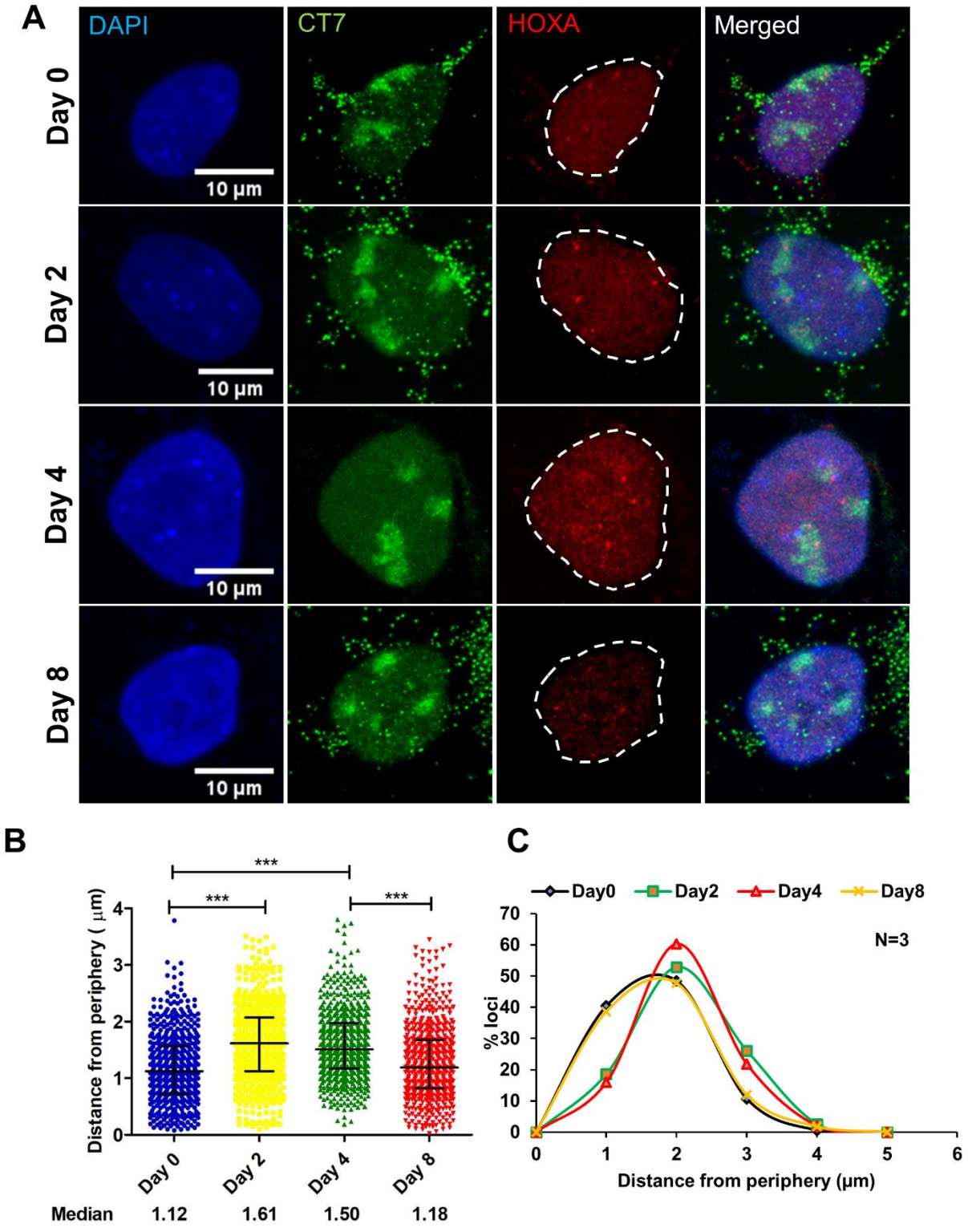

Fig 5: Intranuclear position of HOXA gene cluster during differentiation.

(A)Representative images of NT2/D1 nuclei during differentiation. Chromosome 7 in

green and HOXA locus in red. (B) HOXA locus positioning data pooled from all 3 biological replicates and plotted as scatter for Day 0 (n=537, median=1.12±0.6µm*), 2 (n=548, median=1.61*±0.69µm*), 4 (n=601, median=1.5*±0.62µm*) and 8 (n=621, median=1.18*±0.66µm*). Error bars represent interquartile range. Significance between samples calculated using t test. (*** = p<0.001) (C) HOXA locus positioning data pooled from all 3 replicates and binned into bins of 1µm for all 4 days.*

Nuclear topology during NT2/D1 differentiation

On Day 8, a considerable sub-population of cells with distorted nuclear morphology were observed. Majority of the nuclei showed blebs and are irregular in shape (Fig. 6A). On day 8, ~32% of nuclei showed irregular morphology as compared to Day 0, 2 and 4 with ~4% irregular nuclei (Fig. 6B). Considering the possibility that irregular nuclear shapes may confound the localization of the HOXA gene locus, distorted nuclei were analyzed independently. On Day 8, the distance of the HOXA gene locus was significantly closer to the nuclear periphery in irregular nuclei (median = 0.88µm) as compared to that of regular nuclei (median = 1.4µm) (Fig. 6C). In both regular as well as irregular Day 8 nuclei distance of HOXA locus was lower than that in Day 4 (median = 1.5µm) suggesting movement of loci towards periphery.

To determine the extent of heterogeneity in nuclear shape during differentiation, we also calculated topological parameters of the nucleus, such as sphericity, volume and surface area. While the sphericity was unchanged until day 2 (~0.73), sphericity increased on Day 4 (~0.77) (Fig 6D). However, on Day 8, irregular nuclei showed very low sphericity of ~0.6, whereas regular nuclei showed a marginal decrease (~0.73) as compared to day 4. Nuclear volume increased from 810±274 μm^3 to 1020±313 μm^3 on Day 2 but decreased on Day 4 (792±194 μm^3) and Day 8 (816±255) (Fig. 6E). Surface area showed fluctuations with increase from 565±135μm^2 to 645±114 μm^2 on Day 2 followed by decrease on Day 4 (527±84μm^2) and finally a marginal yet significant increase on Day 8 (587±144 μm^2) (Fig. 6F).

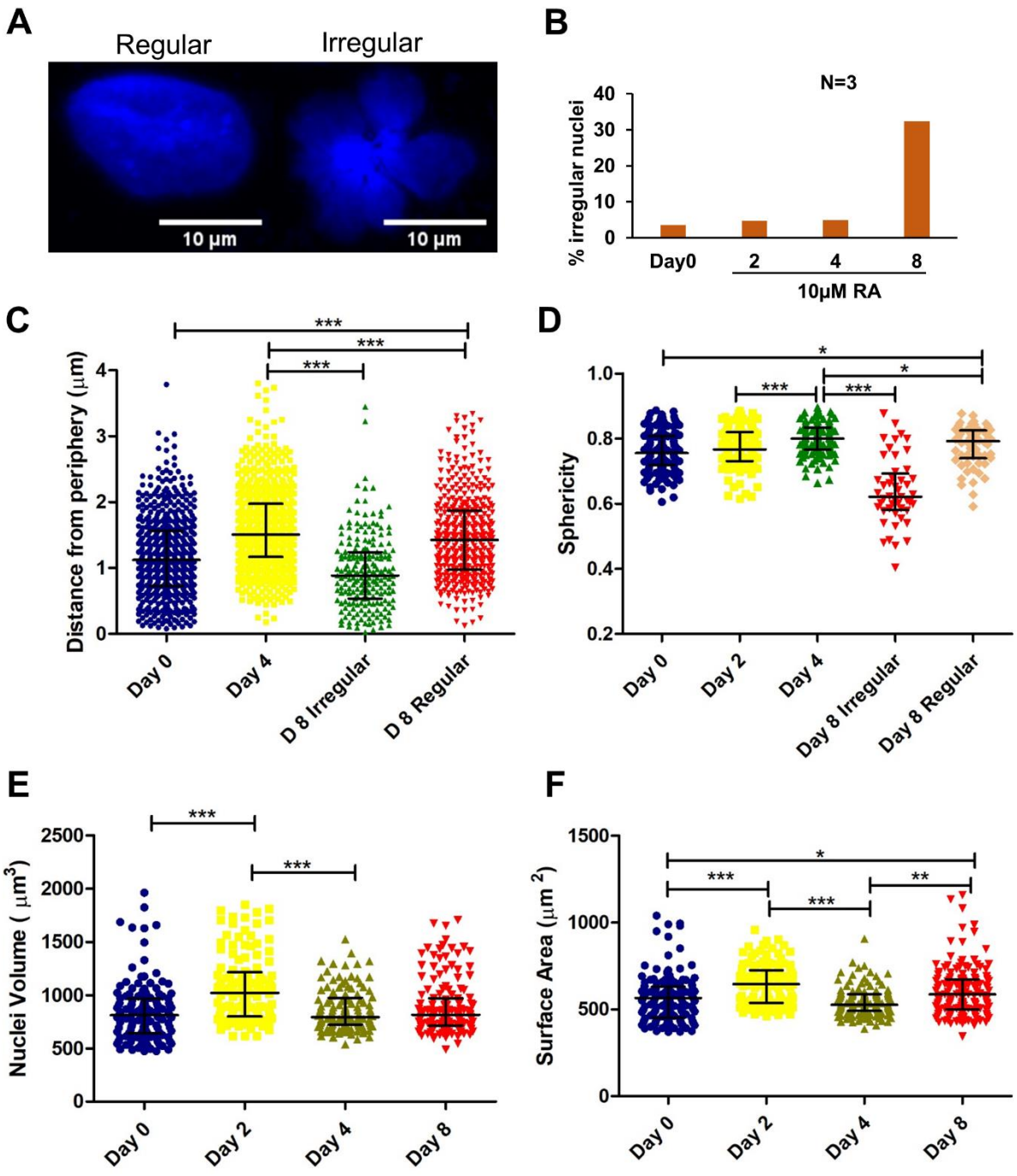

Fig 6: Nuclear topology during NT2/D1 differentiation *(A)Representative images of regular as well as irregular nuclei (B) Percent of irregular nuclei on Day 0 (n= 140),2 (n=125),4 (n=124) and 8 (n=148). Data pooled from 3 biological replicates. (C) HOXA locus positioning data for Day 8 segregated and plotted separately for regular (n=100) and irregular nuclei (n=48). (D) Sphericity of nuclei on Day 0,2,4 & 8. Data for Day 8*

segregated in regular and irregular nuclei. (E) Nuclei volume upon RA treatment (F) Surface area of nuclei upon RA treatment. Data from 3 biological replicates. Significance calculated using Mann-Whitney test. (= p<0.05, ** = p<0.01 *** = p<0.001)*

Levels of Nucleoporins during differentiation

We determined the levels of Nup93 and its interactors during differentiation. Nup93 expression remained unaffected throughout the treatment with a marginal increase on Day 4 (~1.3 fold) (Fig. 7A). Nup188 expression remained constant until Day 4 but decreased on Day 8 (~0.5 fold) (Fig. 7B). Nup205 expression did not show any significant change (Fig. 7C). CTCF expression levels remained constant except for a minor increase on Day 4 (~1.2 fold) (Fig. 7D).

Nup93, Nup188, Nup205 and CTCF levels were variable upon RA treatment but did not show any major changes, as examined by immunoblotting (Fig. 7E,F).

Antagonistic roles of Nup93 and CTCF in HOXA gene expression

Nup93 and its interactors repress HOXA expression (Labade et al). To determine if Nup93 exerts a similar repressive effect on HOXA in cells undergoing differentiation, we examined HOXA levels in NT2/D1 cells. We knocked down Nup93 in undifferentiated cells using siRNA and examined HOXA levels using RT-qPCR. HOXA1 and HOXA5 expression showed ~2 fold increase on Nup93 knockdown (Fig. 8A). However, HOXA9 and HOXA13 showed ~0.5 fold decrease in expression upon Nup93 knockdown (Fig. 8B). When CTCF was knocked down in undifferentiated NT2/D1 cells, HOXA1 and HOXA5 gene expression decreased by~0.5 fold downregulation of HOXA1 and HOXA5 expression was observed in CTCF Kd cells (Fig. 8A). On the other hand CTCF depletion led to an increase in expression of HOXA9 and HOXA13 (Fig. 8B). Thus Nup93 and CTCF knockdown show antagonistic effects on HOXA expression. The combined knockdown of CTCF and Nup93, did not significantly alter expression levels of HOXA genes, as compared to the individual knockdowns. The independent and combined knockdowns of Nup93 and CTCF did not significantly affect the expression levels of pluripotency markers such as Oct4, Sox2 and Nanog (Fig. 8C).

We validated the knockdown of Nup93 and CTCF using western blots (Fig. 8D). Knockdown of Nup93 and CTCF was achieved (Fig. 8E). Nup93 levels were unaffected upon CTCF knockdown. CTCF levels decrease upon Nup93 knockdown (Fig. 8E).

RA treatment upon Nup93 depletion alters HOXA gene expression

To investigate the role of Nup93 in HOXA gene expression during differentiation, cells were treated with RA in a Nup93 depleted background and HOXA gene expression was quantified (Fig. 9A). However considerable cell death was observed upon prolonged knockdown of Nup93 (post 72hrs), due to which Nup93 knockdown was terminated. This implies that Nup93 is essential for cell survival. After ~48 hr knockdown, cells were treated with RA for 24 hrs and RNA was extracted for expression analysis using RT-qPCR (Fig. 9A). As expected, RA treatment showed an increase in expression of HOXA genes (Fig. 9B). Significant variability was observed in RA mediated HOXA gene upregulation across independent biological replicates as compared to control cells (Fig. 9B). Nup93 Kd+ RA showed enhanced upregulation of HOXA1 (Fig. 9B) and HOXA5 than siLacZ + RA samples in all replicates (Fig. 9C). On the other hand, CTCF Kd+ RA led to decrease in expression of HOXA1 when compared to siLacZ +RA (Fig. 9D). HOXA5 expression showed opposite effect across 2 biological replicates (Fig. 9E). Expression levels of 5' HOXA gene were found to be stochastic across replicates (data not shown).

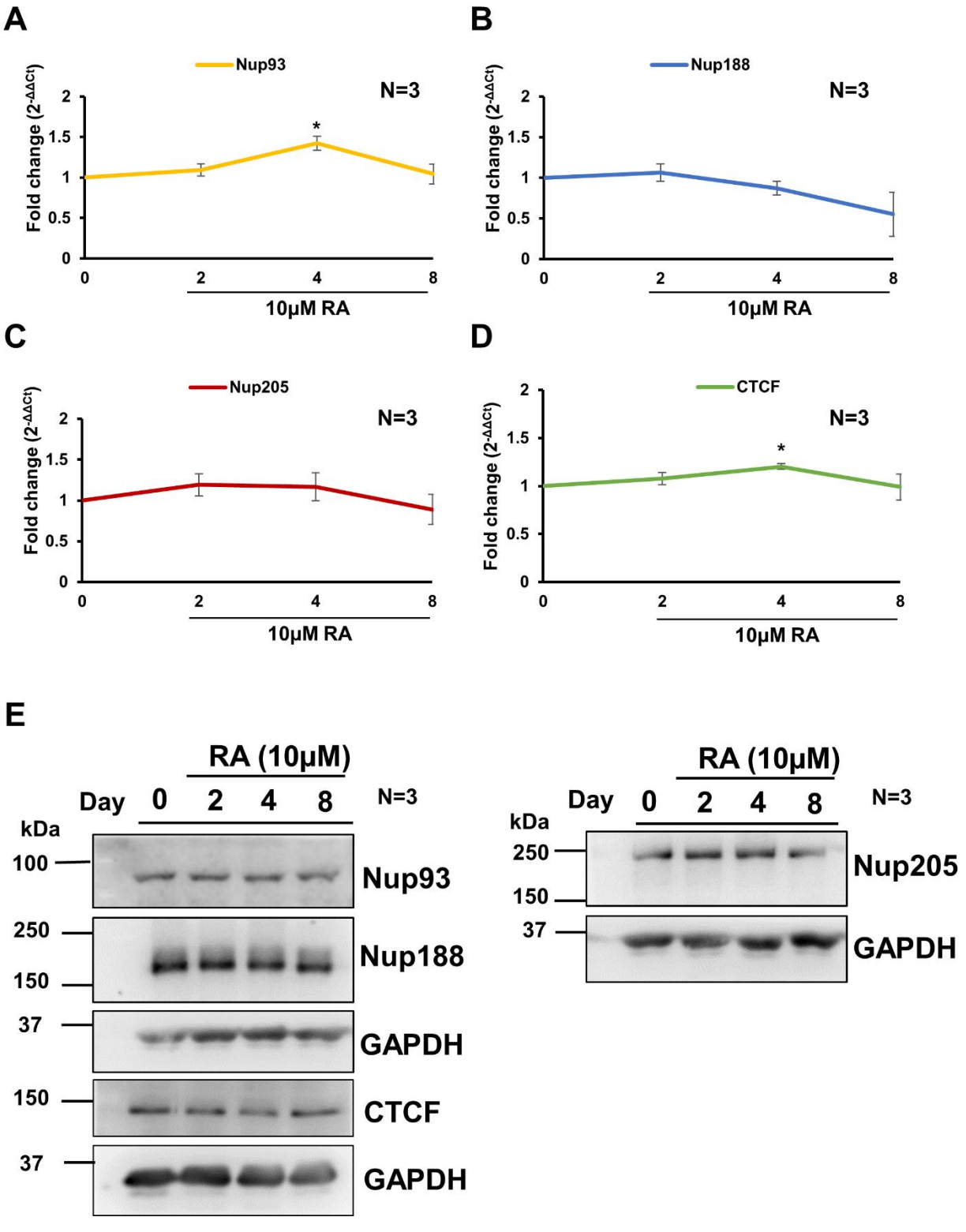
A
Nup93
N=3
Fold change (2-ΔΔCt)
2
1.5
1
0.5
0
*
0
2
4
8
10μM RA
B
Nup188
N=3
Fold change (2-ΔΔCt)
10μM RA
C
Nup205
N=3
Fold change (2-ΔΔCt)
10μM RA
D
CTCF
N=3
Fold change (2-ΔΔCt)
*
10μM RA
E
RA (10μM)
Day 0 2 4 8
N=3
kDa
100
Nup93
250
150
Nup188
37
GAPDH
150
CTCF
37
GAPDH
RA (10μM)
Day 0 2 4 8
N=3
kDa
250
150
Nup205
37
GAPDH

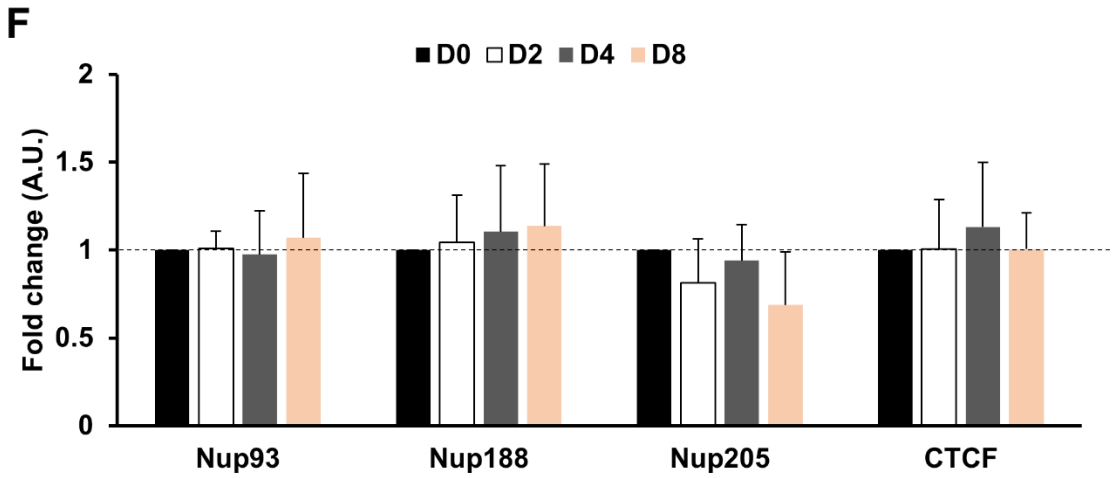

Fig 7: Levels of nucleoporins during differentiation *(A) Nup93 (B) Nup188 (C) Nup205 (D) CTCF expression during differentiation. Date normalized to respective Day 0 samples. Significance calculated using t test (* = p<0.05, ** = p<0.01) (E) Levels of Nup93, Nup188, Nup205, CTCF and Oct4 during differentiation. (F) Quantification of western blots for protein levels. Data from 3 biological replicates. Error bars represent SEM.*

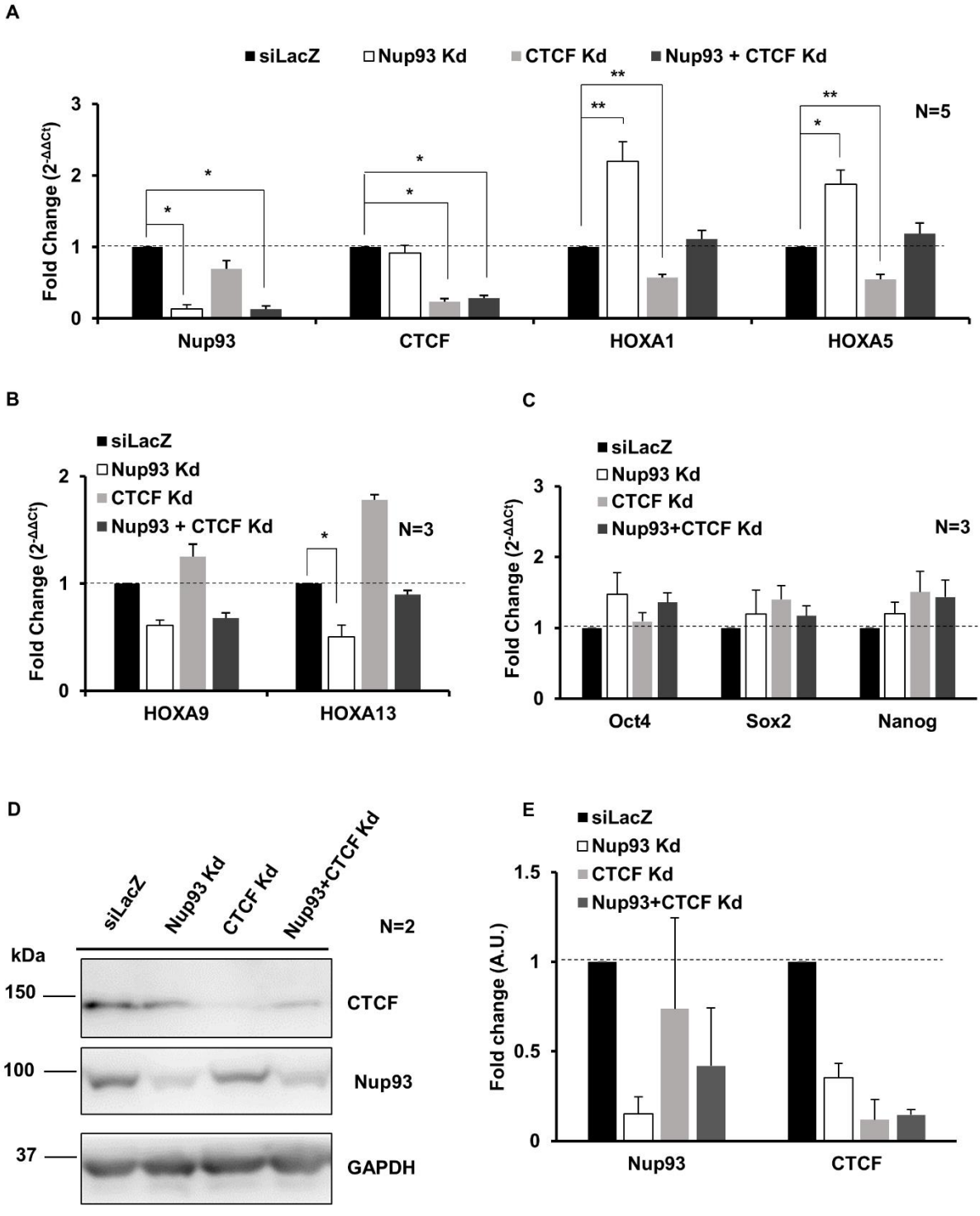
A
siLacZ
Nup93 Kd
CTCF Kd
Nup93 + CTCF Kd
Fold Change (2-ΔΔCt)
N=5
Nup93
CTCF
HOXA1
HOXA5
B
siLacZ
Nup93 Kd
CTCF Kd
Nup93 + CTCF Kd
N=3
HOXA9
HOXA13
C
siLacZ
Nup93 Kd
CTCF Kd
Nup93+CTCF Kd
N=3
Oct4
Sox2
Nanog
D
siLacZ
Nup93 Kd
CTCF Kd
Nup93+CTCF Kd
N=2
kDa
150
100
37
CTCF
Nup93
GAPDH
E
siLacZ
Nup93 Kd
CTCF Kd
Nup93+CTCF Kd
Fold change (A.U.)
Nup93
CTCF

Fig 8: Effect of Nup93 knockdown on HOXA genes expression *(A) HOXA1 and HOXA5 expression upon Nup93 and CTCF knockdown. Data from 5 biological replicates. (B) HOXA9 and HOXA13 expression upon Nup93 and CTCF knockdown. Data from 3 biological replicates. (C) Oct4, Sox2 and Nanog expression upon Nup93 and CTCF knockdown. Data from 3 biological replicates. RT-qPCR data normalized to siLacZ samples. Significance calculated using t test. (* = p<0.05, ** = p<0.01) (D) Representative western blots for Nup93 and CTCF levels upon respective knockdown. (E) Quantification of western blots. Data from two biological replicates. Error bars represent SD.*

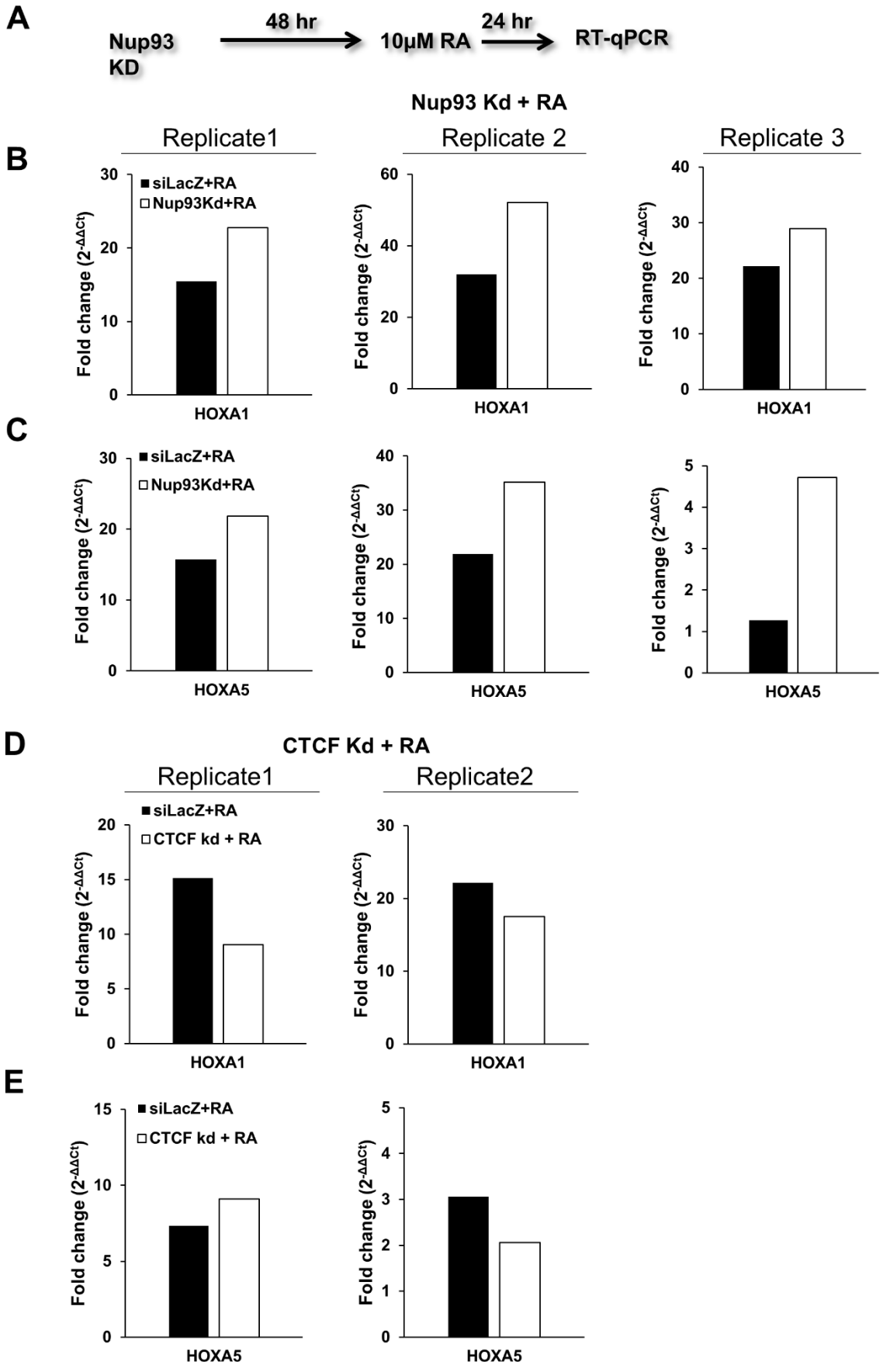
A
Nup93 KD
48 hr
10μM RA
24 hr
RT-qPCR
Nup93 Kd + RA
B
Replicate1
Replicate 2
Replicate 3
siLacZ+RA
Nup93Kd+RA
Fold change (2-ΔΔCt)
HOXA1
C
HOXA5
D
CTCF Kd + RA
Replicate1
Replicate2
siLacZ+RA
CTCF kd + RA
HOXA1
E
HOXA5

Fig 9: Effect of Nup93 and CTCF on HOXA expression during RA treatment. *(A) Schematic of experimental setup. (B) HOXA1 expression in siLacZ + RA and Nup93 Kd+ RA across 3 biological replicates. Data for each replicate normalized to respective siLacZ (not shown). (C) HOXA1 and HOXA5 expression levels in Nup93 Kd+ RA samples. Data from 3 biological replicates and normalized to siLacZ + RA. Error bars represent SEM. Significance calculated using t test (* = p<0.05). (D) HOXA gene expression levels in CTCF Kd+ RA samples. Data from 2 biological replicates and normalized to siLacZ + RA. Error bars represent SD.*

Nup93 and CTCF occupancy within HOXA cluster during RA treatment

We next sought to investigate the mechanisms of Nup93 and CTCF mediated regulation of HOXA expression. Nup93 associates with promoters of 3' HOXA genes (Labade et al. 2016). Similarly, CTCF regulates organization of HOXA locus during differentiation through its association with the HOXA gene cluster (Xu et al. 2014). To examine the role of Nup93 and CTCF in HOXA organization, we performed Chromatin Immunoprecipitation (ChIP) of Nup93 and CTCF followed by RT-qPCR. We determined the occupancy of Nup93 and CTCF at previously reported binding sites (Fig. 10A) on Day 0, 4 and 8 of RA treatment. Nup93 associates with 3' end of HOXA gene cluster (promoters of HOXA1, HOXA3 and HOXA5). In contrast, CTCF associates with 5' end of the HOXA gene cluster (CBS1-5) (Fig. 10A). We detected a decrease in the occupancy of Nup93 at HOXA1 promoter on Day 4 followed by an increase on Day 8 (Fig. 10B). Control regions (~3Kb upstream and downstream of HOXA1 TSS) did not show any binding, supporting the specificity of the pull down (Fig. 10 C,D). Nup93 and CTCF occupancy on HOXA5 promoter decreased with RA treatment (Fig. 10E). Pan H3 (Histone 3) antibody was used as antibody control for immunoprecipitation. PanH3 occupancy on HOXA1 promoter decreased on Day 4 and an increase in occupancy was observed on Day 8 (Fig. 10B). Although Pan H3 occupancy for upstream and downstream regions remained relatively constant, a gradual increase was observed for HOXA5 promoter (Fig. 10E).

CTCF occupancy on CBS in HOXA gene cluster is altered during RA treatment. Similar to previously reported results, CTCF occupancy on CBS1, 2 and 4 was found to decrease upon Day 4 and Day8 (Fig. F,G & H). Pan H3 occupancy on CBS1, 2 remained constant throughout RA treatment whereas Pan H3 binding on CBS4 showed gradual increase with RA treatment.

Effect of Nup188 and Nup205 knockdown on HOXA gene expression

Nup93 regulates HOXA gene expression through its interacting partners Nup205 and Nup188 (Labade et al. 2016). To determine if this mode of regulation is maintained during differentiation, HOXA gene expression was examined upon Nup188 and Nup205 depletion for 48 hours, followed by RA treatment for 24 hours (similar to as described in Fig. 9A). Nup188 knockdown in untreated cells showed a ~50% decrease in expression of HOXA5, HOXA9 and HOXA13 (Fig. 11A). Similar to Nup93 Kd+ RA, considerable variability across biological replicates was observed in RA treated samples. Nup188 Kd+ RA showed an increase in HOXA1 expression as compared to siLacZ + RA (Fig. 11B). However, opposite trends were observed in HOXA5 expression in two biological replicates (Fig. 11B). Nup205 knockdown in untreated cells resulted in decrease in HOXA gene expression (Fig. 11A). RA treatment upon Nup205 Kd showed a decrease in HOXA1 and HOXA5 expression (Fig. 11C). Knockdown of Nup93, Nup188 and Nup205 did not alter expression levels of one another, but for a marginal increase in Nup188 levels upon Nup205 knockdown (Fig. 11D).

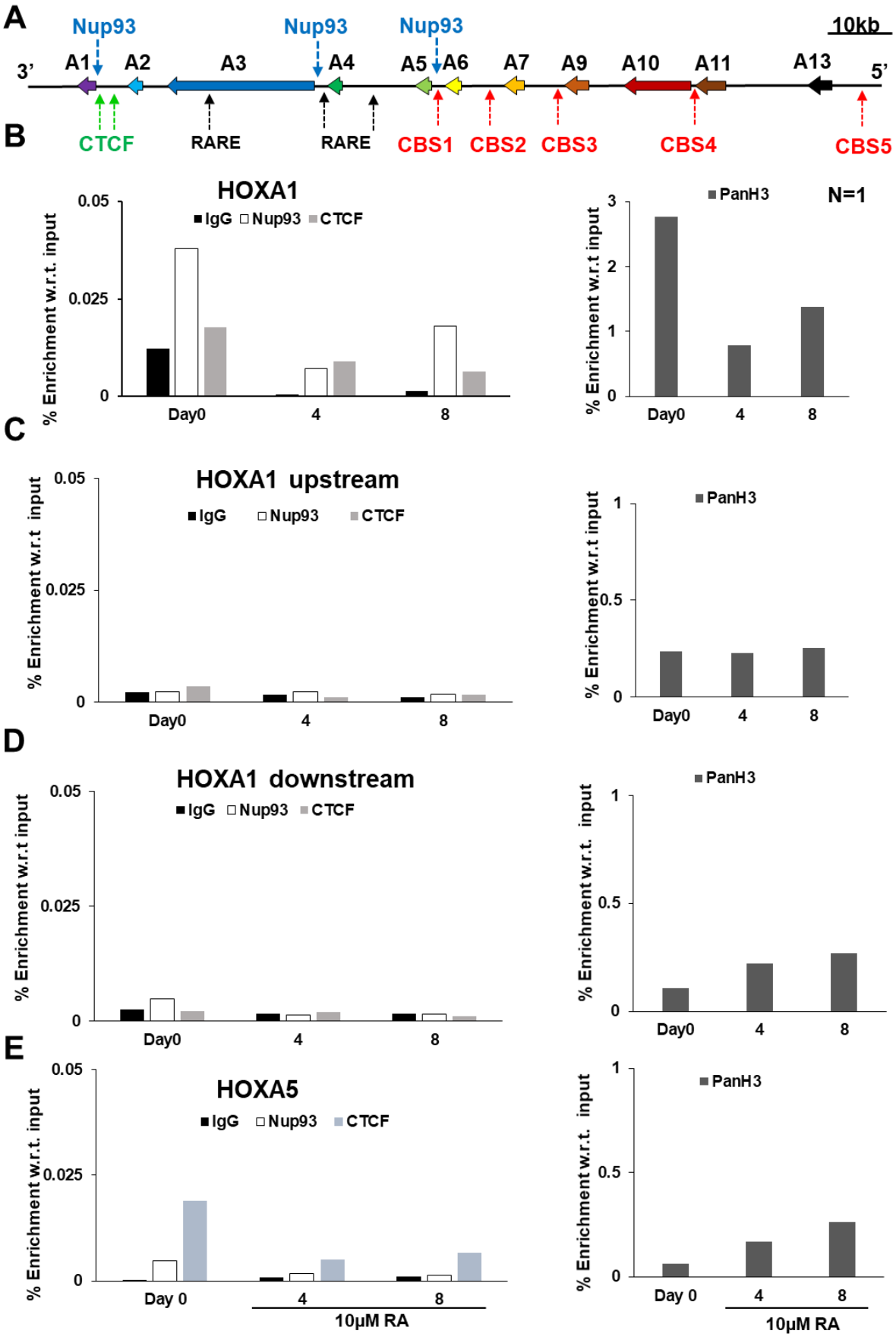
A
Nup93
Nup93
Nup93
10kb
3'
A1
A2
A3
A4
A5
A6
A7
A9
A10
A11
A13
5'
B
CTCF
RARE
RARE
CBS1
CBS2
CBS3
CBS4
CBS5
HOXA1
IgG
Nup93
CTCF
% Enrichment w.r.t input
0.05
0.025
0
Day0
4
8
PanH3
N=1
3
2
1
C
HOXA1 upstream
D
HOXA1 downstream
E
HOXA5
Day 0
10μM RA

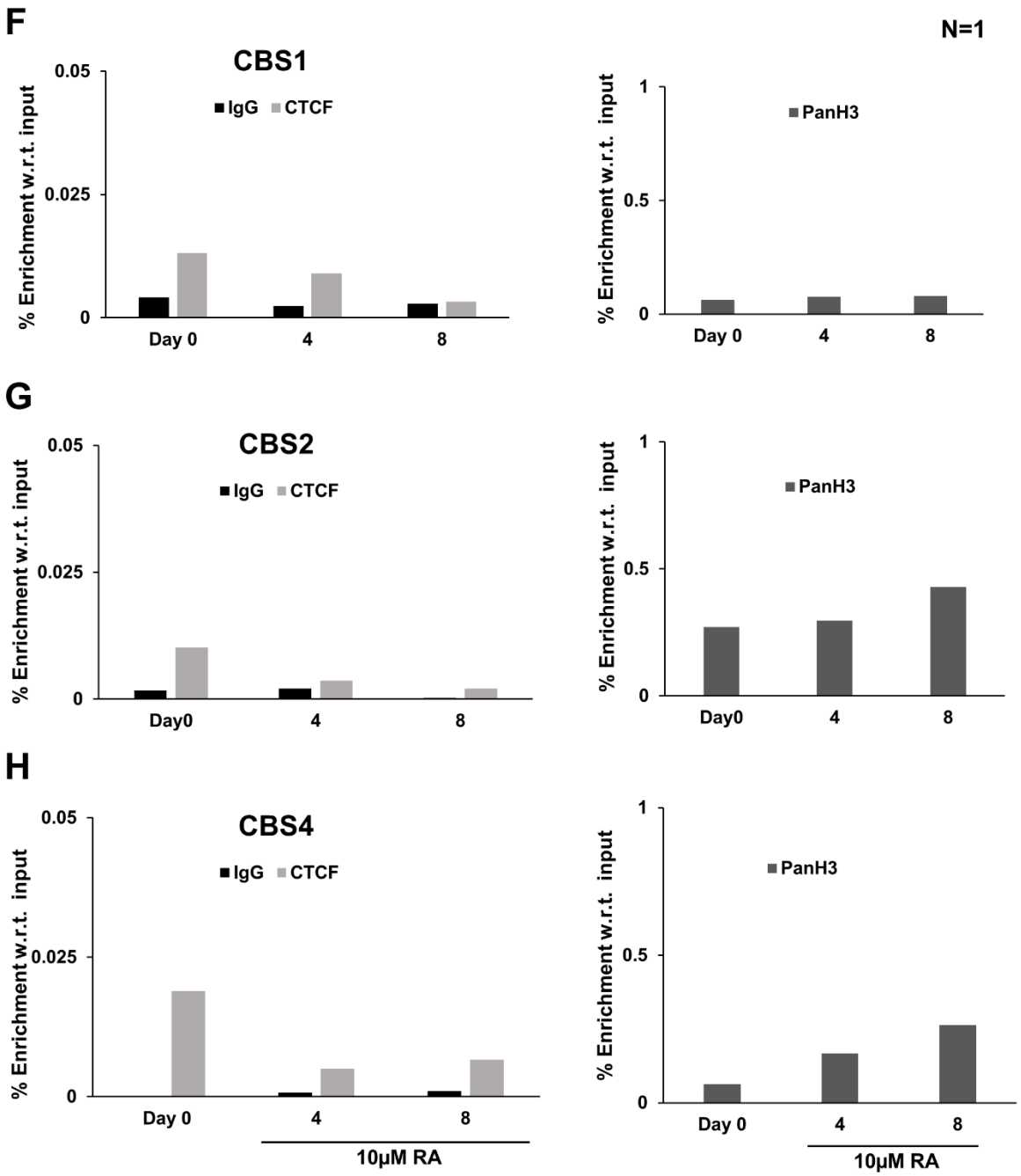

Fig 10: Nup93 and CTCF binding within HOXA gene cluster*. (A) Schematic of Nup93 and CTCF binding sites within HOXA cluster.*

Nup93 and CTCF occupancy on - (B) HOXA1 P2 region (C)~3Kb upstream of HOXA1 promoter (D) ~3Kb downstream of HOXA1 promoter (E) HOXA5 P2 region. (F) CBS1

(G) CBS2 (H) CBS4. Data from one biological replicate (Average of 3 technical replicates). Data normalized to 1% input. Pan H3 used as antibody control.

Organization of Nup93 subcomplex during differentiation

As previously reported, Nup188 and Nup205 interact with Nup93 but not with one another (Labade et al. 2016). However, composition of nuclear pore complex may be altered during differentiation (Raices and D'Angelo 2012). We therefore examined the stability of the Nup93 sub-complex in NT2/D1 cells. We asked if this organization is also maintained in NT2/D1 cells during differentiation. Nup188 was immunoprecipitated and its association with Nup93 and Nup205 was determined using western blotting. Nup188 was found to associate with Nup93 but not with Nup205 and CTCF upon RA mediated differentiation, suggesting that the Nup93 is a stable sub-complex and may not rearrange during differentiation (Fig. 12).

Effect of Nup93, Nup188 and Nup205 knockdown on RNA export

To address if perturbing the Nup93 sub-complex impacts RNA export, we performed RNA FISH upon Nup93, Nup188 and Nup205 knockdown. Transcripts were visualized by fluorescent probes against poly A tails after 48 hr knockdown of respective Nups (Fig. 13A,B). Ratio of nucleoplasmic and cytoplasmic fractions was calculated and compared to control cells. Nup93 knockdown showed a significant increase in nucleoplasmic to cytoplasmic (Nu/Cyt) ratio (median = 1.36) compared to controls (siLacZ, median = 1.0) (Fig. 13C). Nup188 knockdown showed a significant decrease in Nu/Cyt ratio (median = 0.94), while Nup205 knockdown (median = 1.15) did not show a significant change.

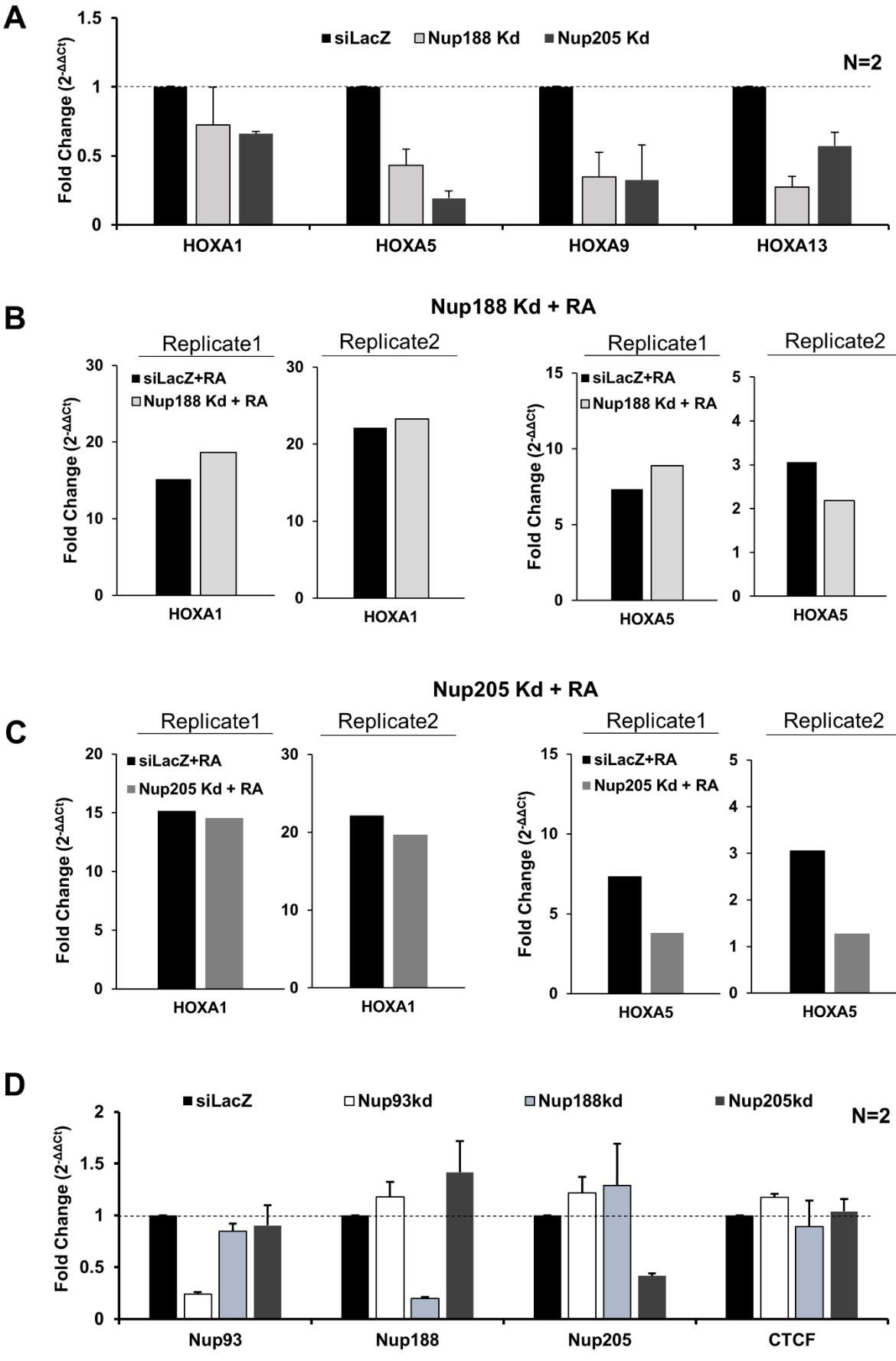
A
siLacZ
Nup188 Kd
Nup205 Kd
N=2
Fold Change (2-ΔΔCt)
HOXA1
HOXA5
HOXA9
HOXA13
B
Nup188 Kd + RA
Replicate1
Replicate2
siLacZ+RA
Nup188 Kd + RA
C
Nup205 Kd + RA
D
Nup93kd
Nup188kd
Nup205kd
Nup93
Nup188
Nup205
CTCF

Fig 11: Effect of Nup188 and Nup205 knockdown on HOXA gene expression during differentiation*. (A) Effect of Nup188 and Nup205 knockdown on HOXA genes. (B) Effect of Nup188 knockdown on HOXA1 and HOXA5 expression during RA treatment. (C) Effect of Nup205 knockdown on HOXA1 and HOXA5 expression during RA treatment. Data normalized to untreated siLacZ. (D) Effect of Nup93, Nup188 and Nup205 knockdown on expression of each other. Total 72 hr knockdown. Data from 2 biological replicates. Error bars represent SD.*

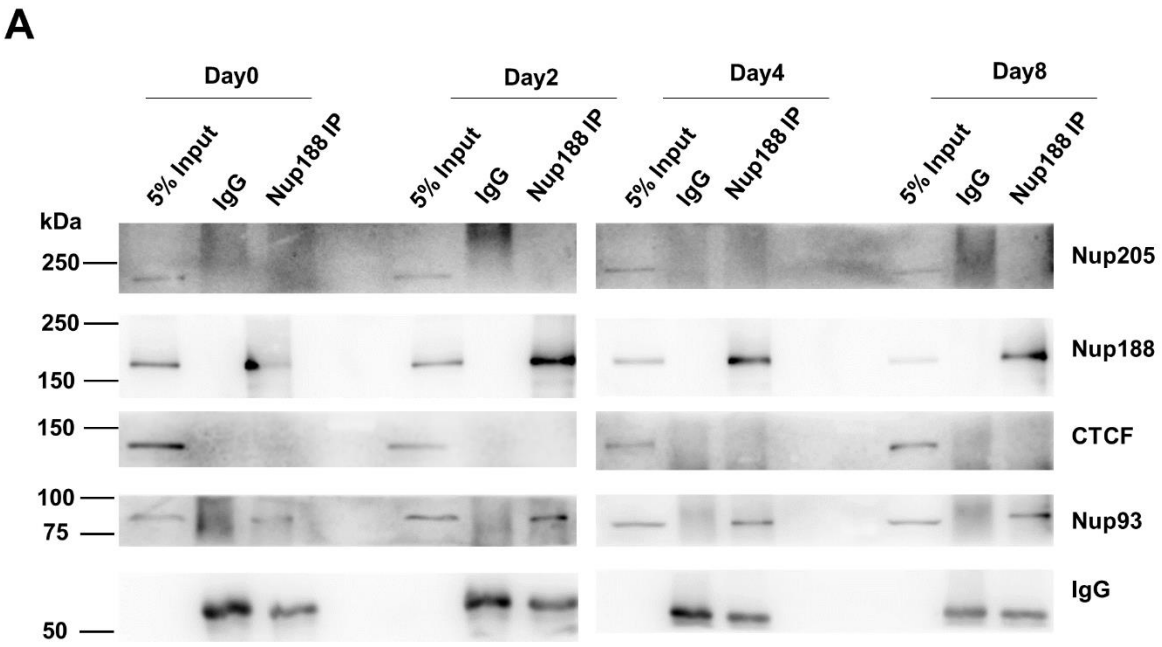

Fig 12: Nup93 subcomplex organization during RA treatment*. Immunoprecipitation was performed with Nup188 antibody and was checked for interaction with Nup205, Nup93 and CTCF. Data from one biological replicate.*

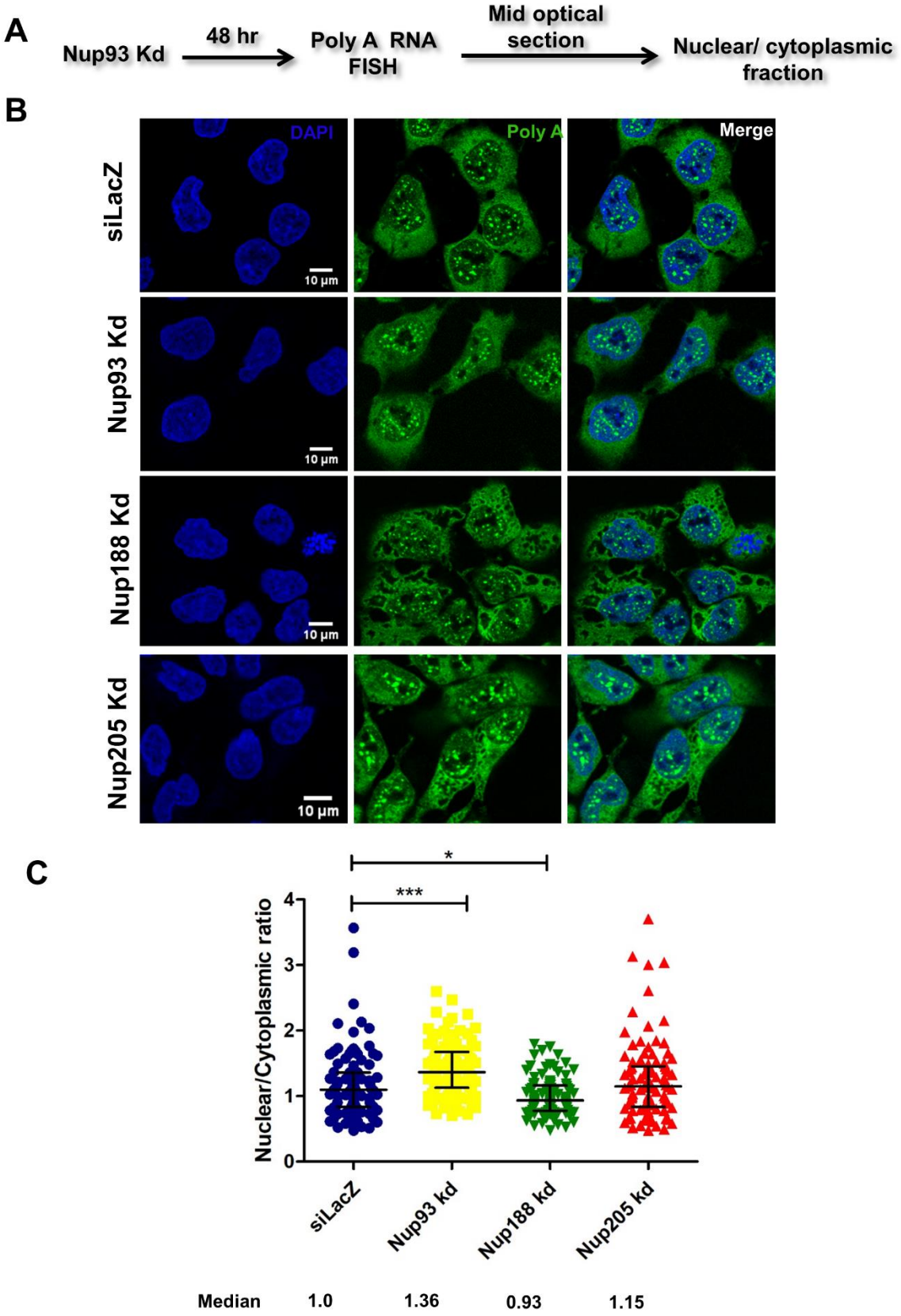
A
Nup93 Kd
48 hr
Poly A RNA FISH
Mid optical section
Nuclear/ cytoplasmic fraction
B
DAPI
Poly A
Merge
siLacZ
Nup93 Kd
Nup188 Kd
Nup205 Kd
10 µm
C
*
***
Nuclear/Cytoplasmic ratio
0
1
2
3
4
siLacZ
Nup93 kd
Nup188 kd
Nup205 kd
Median
1.0
1.36
0.93
1.15

Fig 13: Effect of Nup93, Nup188 and Nup205 knockdown on RNA export *(A) Schematic of experimental paradigm. (B) Representative images of Poly A RNA FISH. (C) Scatter plot comparing Nuclear/ Cytoplasmic ratio of Poly A FISH signal from siLacZ (n= 99), Nup93 Kd (n= 100), Nup188 Kd (n= 100) and Nup205 Kd (n= 96). Data from 1 biological replicate. Error bars represent interquartile range. Significance calculated using Mann-Whitney test.*

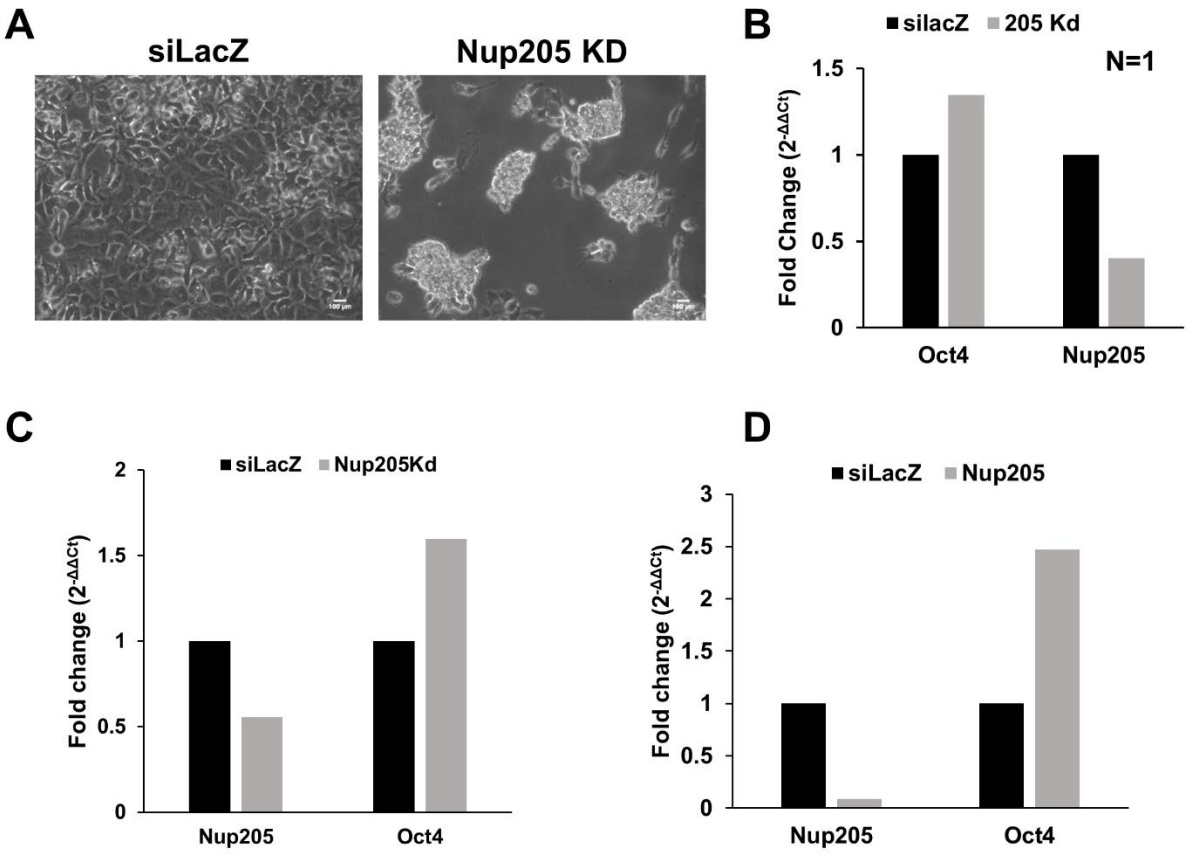

Fig. 14: Effect on Nup205 on Oct4 expression *(A) Morphological changes in NT2/D1 cells upon Nup205 knockdown 72 hrs post transfection. Scale bar = 100µm. (B) Oct4 expression upon 72 hr Nup205 knockdown. (C) Oct4 expression upon 1week Nup205 knockdown. (D) Oct4 expression upon 2 week Nup205 knockdown*

Nup205 knockdown leads to increase in Oct4 levels

Nup205 depleted cells showed change in cell morphology after 72 hrs post transfection. NT2D1 cells showed cell aggregation upon Nup205 knockdown (Fig. 14A). Also in these cells, Oct4 expression was found to increase by ~1.2 fold (Fig. 14B). To determine if prolonged knockdown of Nup205 further increases Oct4 expression, 1 & 2 week knockdowns of Nup205 were performed and Oct4 expression was quantified. One week knockdown of Nup205 resulted in ~1.6 fold upregulation of Oct4 (Fig. 14C). Nup205 knockdown maintained till 2 weeks led to ~2.5 fold upregulation of Oct4. Thus preliminary results suggest that Nup205 represses Oct4 expression.

Discussion

Nucleoporins are structural components of NPCs and are essential for transport of molecules across the nuclear envelope. Along with these functions nups participate in gene regulation and potentially cell differentiation (D'Angelo et al. 2012). Nups associate with and recruit transcription factors and mediate chromatin looping thus influencing gene expression. Mobile nups such as Nup98 are present in the nucleoplasm as well in the NPC. These nups can directly recruit transcription factors and regulate gene expression (Pascual-Garcia et al. 2014). However stable nups such as Nup93, are always present at the NPCs. Here we have elucidated the role of three such stable nups (Nup93, Nup188 and Nup205) in HOXA gene regulation. Previously Nup93 was shown to associate with the promoters of HOXA genes and repress their expression in DLD1 colorectal carcinoma cells by potentially tethering HOXA locus to the nuclear periphery. Nup93 exerts these effects assisted by Nup188 and Nup205 respectively (Labade et al. 2016). These findings suggest potential mechanisms by which stable nups regulate gene expression. Nup93 binds to super-enhancers which regulate expression of cell identity genes (Ibarra et al. 2016). Also, ChIP-seq data analyses predicted a potential role for Nup93 in differentiation (unpublished data). These results implicate Nup93 as regulator of differentiation. We sought to examine how Nup93 affects HOXA gene expression during differentiation. NTera2.D1 embryonal carcinoma cells when treated with RA, differentiate into a neuronal lineage. HOXA gene expression is upregulated during differentiation (Xu et al. 2014). Our results corroborate these reports and show collinear expression of HOXA gene in response to RA. Such a pattern of collinearity is characteristic of HOX genes and is a confirmation of the Retinoic Acid (RA) response. Relative expression levels HOXA5 and HOXA9 upregulation was found to be higher than HOXA1 (Fig. 4). This can be attributed to differential response of promoters of the genes to RA. Decrease in expression of pluripotency markers (Oct4, Sox2 and Nanog) proved that NT2/D1 cells are differentiating (Fig. 3). Increased expression of Pax6 ensured that cells are differentiating into the neuronal lineage. Expression as well as protein levels of Nup93, Nup188, Nup205 and CTCF were stable throughout the RA treatment. Consistent with

this, the association of Nups was unchanged upon RA treatment. Nup188 was found to interact with Nup93 but not Nup205, as previously shown (Labade et al. 2016).

Position of HOXA gene cluster was found to change during RA treatment. NT2/D1 cells harbor 4 copies of HOXA cluster (unpublished data). Indeed 4 copies of HOXA cluster were detected in FISH. In initial repressed state, HOXA locus is present at nuclear periphery. With RA mediated induction, HOXA was re-positioned towards the nuclear interior which favors expression, resulting in high levels of upregulation. By Day 8, consistent with a decrease in expression of 3' HOXA genes, HOXA genes showed a movement towards nuclear periphery. However the probe used for visualization is made from BAC (bacterial artificial chromosome) and detects all HOXA genes and thus fails to capture a more detailed dynamics within the cluster. Probes specific to different genes within the cluster can provide more insights into localization of genes and whether it correlates with their expression. In a subpopulation of highly irregular nuclei (- Day 8), HOXA gene loci positioned closer to the nuclear periphery than regular nuclei. This may be due to the highly irregular shape of these nuclei which might affect the measurement or possible difference in differentiation status of these cells. The precise reason behind this effect is still unclear. This subpopulation was found to have very low nuclear sphericity when compared to normal cells. Overall sphericity was found to increase with RA treatment. Nuclear volume showed fluctuations, with increase on Day 2 followed by decrease on Day 4 onwards. Even though volume change was observed, since absolute distance of loci from nearest DAPI edge was calculated and was not normalized to any other parameter, loci measurement remains unaffected.

Nup93 knockdown revealed interesting patterns of regulation where 3' HOXA genes (HOXA1 and HOXA5) showed upregulation but 5' HOXA genes (HOXA9 and HOXA13) showed downregulation in untreated cells. This result clearly shows two opposing roles of Nup93 in regulation of two parts of the gene cluster. However, HOXA1 and HOXA5 gene expression was found to decrease upon CTCF knockdown whereas HOXA9 and HOXA13 expression increased upon CTCF knockdown producing the exact opposite pattern of regulation as shown by Nup93. This type of pattern might result because of the organization of HOXA cluster. HOXA gene cluster is known to be organized in two segments (3' and 5' respectively) which are separated by CTCF binding sites

(Rousseau et al. 2014). Deletion of CBS1 was shown to result in disruption of TAD (topologically associated domains) boundary and increased chromatin contacts between two parts of the cluster (Narendra et al. 2015). These studies together underline the role of CTCF in maintaining HOXA cluster in two segments, with different regulatory mechanisms in two different parts of the HOXA gene. Since CTCF binding sites are present on 5' region of the cluster, CTCF depletion might lead to loss of chromatin loops, thereby facilitating transcription. It was observed that Nup93 knockdown increased occupancy of CTCF on CBS (unpublished data). This is further reflected in the downregulation of 5' HOXA genes upon Nup93 knockdown. Nup93 depletion allowing increased CTCF occupancy could result in increased chromatin compaction, thereby leading to decrease in expression. These results suggest possible role of Nup93 in chromatin looping in 3' part of the cluster. Through such mechanisms, Nup93 and CTCF might contribute to regulating 3' and 5' part of the cluster, respectively. We further asked if this regulation is maintained during RA treatment. Surprisingly, as opposed to the undifferentiated cells, RA treatment upon Nup93 knockdown, shows considerable variability across biological replicates. As argued by Rousseau et al, such variability may be attributed to the innate heterogeneity in untreated cells (Rousseau et al. 2014). Indeed after normalization to untreated control, levels of HOXA gene upregulation differ considerably across replicates. However, when RA treated control and knockdown samples are compared, it was found Nup93 knockdown enhanced upregulation of HOXA genes. This indicated that Nup93 knockdown confers responsiveness to the 3' HOXA genes as compared to RA treatment. RA treatment in CTCF depleted cells showed decreased HOXA1 expression. The stochasticity in 5' HOXA gene expression could be attributed to sensitivity of RA treatment as well as temporality of HOXA upregulation. Loss of CTCF binding on 5' part of HOXA cluster facilitates expression on genes (Xu et al. 2014). Since RA treatment evicts CTCF from its binding sites (Ishihara et al. 2016) this process itself is subject to variability in RA treatment. Therefore minor changes in time of sample collection might lead to amplification of such variability, resulting in different results across replicates. Hence no conclusive results could be drawn for 5' HOXA genes during RA treatment.

Nup93 binding on HOXA1 and HOXA5 promoter negatively correlates with their expression during RA treatment suggesting direct role of Nup93 in repression through binding to promoters. Nup93 ChIP results also support the HOXA positioning data with maximum occupancy on Day 0 and Day 8, when the loci was closer to the periphery. CTCF binding on HOXA1 promoter decreases during RA treatment, prompting its role in facilitating HOXA1 expression. This positive regulatory role is also underlined by knockdown experiments mentioned above. Similar to previous reports, CTCF binding to CBS present on 5' part of the cluster decreased with RA treatment consistent with upregulation of 5' genes. Together these results reveal an interplay between Nup93 and CTCF in regulating different parts of the HOXA gene cluster (Fig. 15).

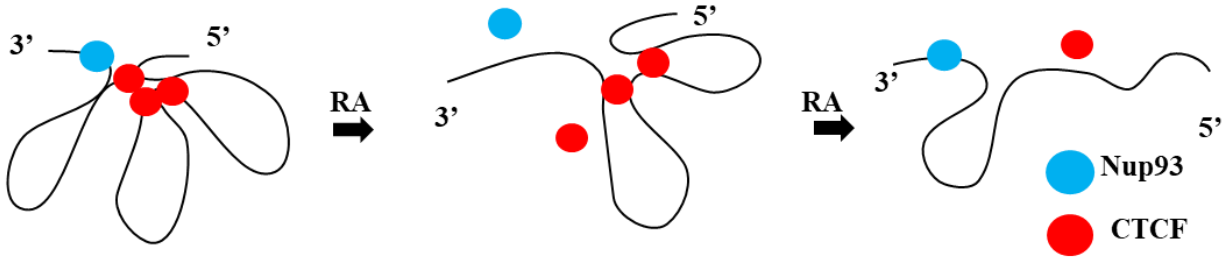

Fig. 15: Nup93 and CTCF binding during RA treatment. *Initially Nup93 and CTCF bind on 3' and 5' part of the cluster respectively. Upon RA treatment Nup93 binding decreases and CTCF occupancy on 5' side starts decreasing. Subsequently, CTCF binding is lost from 5' part while Nup93 contacts 3' gene promoter again.*

Nup93 is known to repress HOXA genes through Nup205 and Nup188 in DLD1 cells. Accordingly Nup188 and Nup205 knockdown results in HOXA gene upregulation (Labade et al. 2016). However, in NT2/D1 cells, Nup188 and Nup205 depletion led to decrease in HOXA genes in undifferentiated cells. Also RA treatment in Nup188 Kd cells enhanced HOXA1 expression. On the other hand Nup205 Kd+ RA leads to decrease in HOXA expression. These results differ from those observed in Nup93 knockdown conditions suggesting independent regulatory mechanisms by these Nups as opposed to DLD1 cells. This suggests that Nup93 does not depend on Nup188 or Nup205 for HOXA gene regulation in NT2/D1. Taken together, these results suggest that in undifferentiated NT2/D1 cells Nup93 binds to 3' HOXA genes, positioning it to

nuclear periphery (Fig. 16). In this state HOXA locus is maintained in looped structure predominantly by CTCF. Upon RA treatment, loci move away from periphery. Accordingly, Nup93 occupancy is lost leading to expression of 3' genes. Subsequently CTCF occupancy on 5' part of cluster is lost resulting in opening of chromatin and expression of 5' genes. Consistent with collinearity, after initial upregulation, 3' HOXA gene expression starts receding accompanied by binding of Nup93 which results in peripheral relocalization of HOXA gene cluster. However, 5' genes still remain active. Nup93 subcomplex organization remains unaltered during RA treatment (Fig. 16).

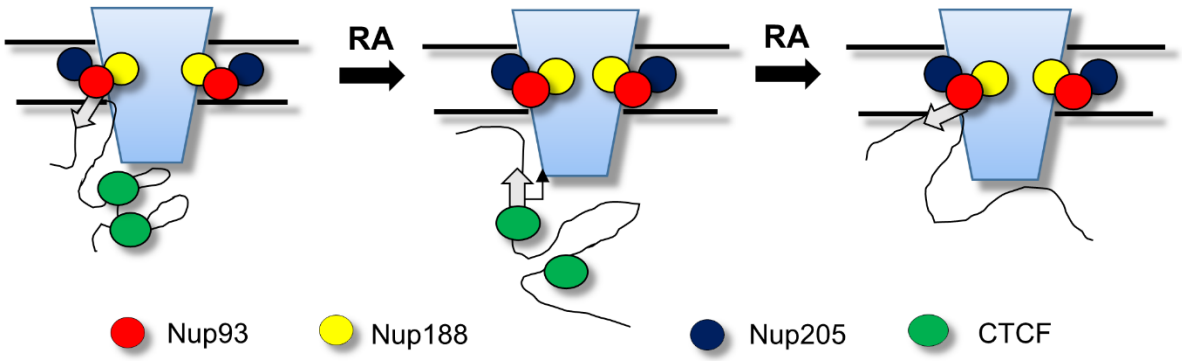

Fig 16: Model for HOXA gene regulation during RA treatment. *Positioning of HOXA gene cluster changes during RA treatment. Nup93 binding localizes HOXA genes to periphery. CTCF occupancy is altered during differentiation. Nup93 subcomplex organization remains constant during differentiation.*

Since Nup93 knockdown led to impaired export of RNA, transport related effects of Nup93 cannot be ignored. Such defects might lead to aberrant transport of regulatory molecules or transcripts, affecting gene expression. Hence contributions of transport related functions and physical binding of Nup93 in HOXA gene regulation remains unknown. Similarly, Nup188 knockdown also enhances RNA export, raising same questions about mechanism of Nup188 mediated regulation.

Surprisingly, Nup205 knockdown showed an increase in Oct4 expression, suggesting a possible role of Nup205 in regulating pluripotency. Cells also showed aggregates similar

to embryoid bodies. Embryoid bodies are 3 dimensional structures arising from spontaneous differentiation of Embryonic Stem cells (Kurosawa 2007). Since Nup205 knockdown did not affect RNA export, it is possible that Nup205 regulates gene expression through mechanisms similar to Nup93. However, since import of proteins upon Nup205 knockdown was not examined, the possibility of defective import leading to downstream effects cannot be ignored. Nevertheless this phenotype can be further explored to check if cells are becoming more pluripotent and can be differentiated into other lineages.

Future directions

To determine if Nup93 binding tethers it to nuclear periphery, position of HOXA locus upon Nup93 depletion should be examined using FISH. Movement of HOXA locus away from periphery upon Nup93 knockdown will establish Nup93 as a tether which contribute to HOXA gene repression through its peripheral positioning. This combined with Nup93 occupancy will further explain mechanism of Nup93 mediated HOXA gene regulation during differentiation. Also mechanism of Nup205 and Nup188 mediated HOXA regulation is still unclear. Since depletion of both showed decrease in HOXA gene expression, it suggests that Nup93 acts independent of its interacting partners. Nevertheless, some aspects of Nup93 mediated gene regulation still remain unclear. Nup93 is a stable nucleoporin and is always found at nuclear periphery. Despite this fact, Nup93 was found to bind to all chromosomes except X chromosomes (unpublished data). How Nup93 contacts chromosomes present away from periphery (e.g. Chr.19) is still elusive. Also Nup93 is embedded within the scaffold of NPC (Fig. 1) making it difficult to directly contact DNA. This hints towards the possibility that Nup93 might acquire these contacts before NPC formation. During post mitotic NPC formation, nucleoporin ELYS contacts chromatin followed by recruitment of Nup107/160 complex (Capelson et al. 2010). Subsequently other scaffold nucleoporins are recruited. It is possible that at this stage, Nup93 is recruited and acquires chromatin contacts, before complete NPC formation. Further addition of nups leads to formation of complete NPC.

However, Nup93 does not harbor any reported or predicted DNA binding motif (InterPro database). Therefore it is possible that Nup93 binds to DNA through an external intermediate or through its interactors (Fig. 17). Such a hypothesis definitely raises a question on efficiency of transport through such NPCs. Therefore how Nup93 binds to DNA still remains unanswered.

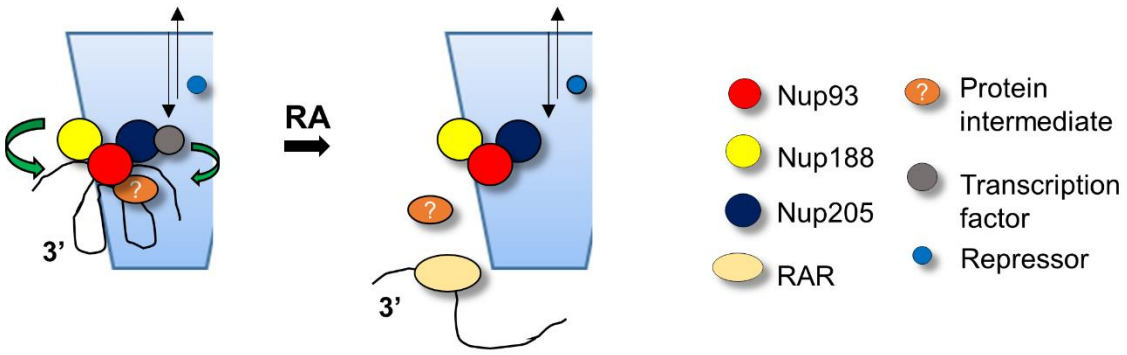

Fig 17: Speculative mechanism of regulation of HOXA genes by Nup93 subcomplex. *Nup93 contacts chromatin either directly or through a protein intermediate and assist in maintaining the organization of the 3' part of the HOXA gene cluster. Also Nup188 and Nup205 may potentially associate with transcription factors that in turn regulate HOXA expression. Independent of this paradigm, is the role of the Nup93 sub-complex in regulating nuclear transport that could further contribute to HOXA gene regulation. Upon RA treatment, Retinoic Acid Receptor (RAR) binds to RARE elements and leads to loss of Nup93 occupancy, resulting in relocalization and upregulation of HOXA genes.*

Materials and Methods

Cell culture

NT2/D1 cells were cultured in Dulbecco's Modified Eagle's Medium supplemented with 10% FBS (Sigma F2442), 100U/ml Penicillin/100µg/ml streptomycin and 2mM Glutamine at 37^{o}C and 5% CO_2. Cells were trypsinized (0.05% trypsin) and subcultured when confluent. Retinoic acid (Sigma R2625) was dissolved in DMSO and was directly added to the medium. RA is light sensitive and was handled in conditions of reduced light. For all experiments, 10µM Retinoic acid was used and was replenished every 2 days. All retinoic acid additions were after 24 hrs of initial cell seeding unless otherwise specified. Untreated cells were collected at Day 0. For prolonged Nup205 knockdown experiments, cells were reseeded every 6 days to maintain the efficiency of the knockdown.

Transient siRNA mediated knockdown

0.2 x 10^6 cells were seeded in 35mm dish and 24 hr after seeding, siRNA transfection was set up. 4µl RNAiMax transfection reagent mixed with 250µl OptiMEM was added to siRNA (Nup93- 20nM, Nup188- 20nM, Nup205- 50nM, CTCF- 50nM) mixed with 250µl OptiMEM. After 30 min incubation this mixture was added to 1.5ml medium to achieve final concentration. As control siLacZ (Dharmacon) was used. Medium was changed 24 hr post addition.

siRNA Oligo sequence-

Nup93- 5'AGAGTGAAGTGGCGGACAA3′

Nup188- 5′GCCTTTCTGCGCTTGATCACCACCC3′

Nup205- 5′AGAUGGUGAAGGAGGAAUAUU3′

CTCF- 5′CAAGAAGCGGAGAGGACGA3′

RNA extraction and cDNA synthesis

Cells were collected in Trizol and vortexed for 15 seconds. 100µl chloroform per 500µl Trizol was added and mixed by vigorous vortexing. After 15 min incubation, samples were spun down at 4^{o}C for 15 min at 12000g. Aqueous layer was separated and equal

volume of Isopropanol was added. Samples were mixed by shaking and incubated for 15 min at RT and spun down at 4ºC/12000g/15 min. Pellet was washed once with 75% ethanol at 4ºC/12000g/15 min. RNA pellet was dried and resuspended in Nuclease free water (Sigma). Quality of RNA was checked on NanoDrop with 1µl RNA. 1µg of RNA was used to prepare cDNA using Verso cDNA synthesis kit in 20µl reaction.

RNA mix

RNA	1µl (1µg)
Oligo dT	1µl
NFW	3µl

Verso Reverse Transcription mix

Reagent	Volume (µl)
5x cDNA Synthesis buffer	4
dNTP mix	2
Verso RT enhancer	1
Verso Enzyme mix	1
Nuclease free water	7

RNA mix was heated at 70ºC for 5 min and quickly chilled in ice for 5 min. 15µl RT mix was added to RNA mix. PCR scheme used for cDNA Synthesis is as follows-

Temperature (ºC)	Time (min)
25	5
42	60
70	5
4	hold

Prepared cDNA was diluted 1:1 with NFW. RT-qPCR was setup with KAPA SYBR Green with 5µl reaction (2.5µl KAPA SYBR, 1.3µl NFW, 0.2µl primer mix, 1µl cDNA). PCR was performed on BIORAD real time PCR. Ct values for each sample were double normalized to internal control and reference, respectively.

Western Blotting

Cells were scraped in RIPA buffer (50 mM Tris–Cl pH 7.4, 150 mM NaCl, 0.1% SDS, 0.1% sodium azide, 0.5% sodium deoxycholate, 1 mM EDTA, 1% NP-40, 1X protease inhibitor cocktail). Lysate was centrifuged at 13000g at 4^{o}C for 10 min. Protein content was quantified using BCA assay (cat. No. 23225). Samples were prepared in 1x Laemmli buffer (Tris– HCl pH 6.8, 2% SDS, 20% glycerol, 0.2% bromophenol blue, 0.025% β-mercaptoethanol) and 20µg protein was loaded. Protein samples resolved by SDS-PAGE were transferred to polyvinylidine fluoride membrane then blocked using 5% skimmed milk in 1X TBST (Tris buffer saline, 0.1% Tween 20) for 1hr at RT. Primary antibodies were diluted in 0.5% milk in 1X TBST and were incubated overnight. Secondary antibodies were diluted in 0.5% milk in 1X TBST. Blots were developed using enhanced chemiluminescence detection reagents (ECL prime and femto). Images were acquired every 10s of exposure.

Fluorescent In Situ Hybridization (FISH)

Cells were washed with 1X PBS and treated with cytoskeleton (CSK) digestion buffer (0.1 M NaCl, 0.3 M sucrose, 3 mM $MgCl_2$, 10 mM PIPES (pH 7.4), 0.5% Triton X-100) on ice. Duration of CSK digestion is variable across different days, as more time was needed to digest the cytoskeleton in differentiated cells. Cells were fixed using 4% Paraformaldehyde (PFA, pH=7.4) for 10 min at RT. Cells were permeabilized with 0.5% TritonX-100 for 10 min at RT. After 1 hr incubation at RT, cells were subjected to 4 cycles of freeze-thaw in liquid nitrogen. Cells were treated with 0.1N HCl for 15 min and washed 3 times with 1X PBS. Cells were stored in 50% Formamide (FA)/ 2X saline sodium citrate (SSC) (pH=7.4) at 4^{o}C. Cells were hybridized with 2µl of human chromosome 7 paint and 2µl of nick translated BAC DNA of HOXA cluster. Coverslips were incubated for 48 hrs in humidified chamber at 37^{o}C. Post hybridization, coverslips

were washed with 50% FA/2X SSC at 45^{o}C thrice followed by 3 washes of 0.1X SSC at 60^{o}C. DAPI staining was performed for 5 min at RT and coverslips were washed once with 2X SSC (pH =7.4). Coverslips were mounted in Slowfade Gold Antifade. Images were acquired using confocal microscope at 63X zoom. Analysis was performed using Huygens Professional Software. After 3D reconstruction of images, distance of each loci from DAPI edge was calculated. Data from 3 independent biological replicates was pooled and statistical analyses was performed using student's t test. Pooled data was also binned in 1µm bins for each time point and the data was plotted.

Poly A RNA FISH

Post fixation cells were treated with 95% methanol for 1 hr at -20^{o}C followed by 5 min treatment with chilled 100% methanol on ice. Cells were washed twice with 2X SSC (pH 7.4) containing VRC (Vanadyl Ribonucleoside Complex) for 5 min at RT. Coverslips were hybridized with hybridization mix (40% formamide, 10% dextran sulfate,0.1 mg salmon sperm DNA and 5 ng/ml of FAM oligo dT prepared in 2× SSC solution) for 3 hr at 37^{o}C. After hybridization, coverslips were washed twice with 2X SSC at RT followed by 0.2X SSC wash. Cells were stained with DAPI and after 1X PBS wash coverslips were mounted. Mid optical sections were imaged and nuclear and cytoplasmic signal was quantified. Nuclear to cytoplasmic ratio was compared using GraphPad Prism software.

Immunoprecipitation

Cells were grown in 100mm dish and harvested on respective days. After 1 wash with 1X PBS cells were scraped in 1 ml cold CoIP lysis buffer (50mM Tris, 0.5% NP40, 150 mM NaCl, 1X PIC and adjusted to pH 8). After incubation on ice for 15 min extracts were centrifuged at 14000 rpm for 15 min at 4^{o}C. Pre-clearing of extracts was performed using 5µl Protein A dynabeads for 30 min at 4^{o}C on fixed rotor. 2µg antibody was incubated with 15µl Protein A dynabeads in 500µl 1X PBST (0.1% Tween 20 in 1X PBS) for 1 hr at 4^{o}C. After pre-clearing, protein content was quantified using BCA assay and 500µg protein was added to antibody coated dynabeads and incubated overnight at

4^{o}C on fixed rotor. Dynabeads were washed 9 times with CoIP lysis buffer. Samples for western prepared in Laemmli buffer.

Chromatin Immunoprecipitation and RT-qPCR

NT2/D1 cells (~4X10^{7}) were crosslinked using 1% Formaldehyde for 10 min at RT. Cross-linking was quenched using 150mM glycine for 5 min and cells were lysed in 1ml swelling buffer (25 mM HEPES pH 8.0, 1.5 mM MgCl2, 10 mM KCl, 0.1% NP-40, 1X PIC). Nuclei were collected by centrifugation at 2000 rpm for 10 min at 4^{o}C. Nuclei were resuspended in 1ml sonication buffer (50 mM HEPES pH 8.0, 140 mM NaCl, 1 mM EDTA, 1% Triton-X-100, 0.1% sodium deoxycholate and 0.1% SDS) and sonication was performed on Bioruptor Twin Sonicator (Diagenode) till chromatin fragments of ~100-500bp were obtained. Sonicated chromatin was pre-cleared by protein A dynabeads at 4^{o}C for 1hr. Chromatin Immunoprecipitation was setup with 100µg of chromatin and 2µg of respective antibody at 4^{o}C overnight. Pre-blocked (1% BSA/ 1X PBS) ProteinA dynabeads were added equally to all samples and incubated for ~4 hrs at 4^{o}C. Beads were then washed with 1ml sonication buffer thrice followed by 3 washes of wash buffer A (50 mM HEPES pH 8.0, 500 mM NaCl, 1 mM EDTA, 1% Triton X-100, 0.1% sodium deoxycholate and 0.1% SDS), wash buffer B (20 mM Tris–HCL pH 8.0, 1 mM EDTA, 0.5% NP-40, 250 mM LiCl, 0.5% sodium deoxycholate and 1× PIC) and TE buffer each at 4^{o}C. Chromatin was eluted in elution buffer (50 mM Tris-HCL pH 8.0, 1 mM EDTA, 1% SDS, 50 mM NaHCO3) and de-crosslinked at 65^{o}C overnight. After RNAse A (20µg, 1hr at 37^{o}C) and Proteinase K (10µg, 1 hr at 65^{o}C) treatment DNA was extracted using Phenol/Chloroform/ Isoamyl alcohol (25:24:1) and precipitated using 3M sodium acetate and glycogen (2µg). DNA samples were resuspended in 20µl NFW. RT-qPCR was performed and quantified using % input method.

Immunofluorescence Assay

Cells were washed with 1X PBS thrice and then fixed with 4% PFA for 10 minutes at RT. Cells were permeabilized with 0.5% TritonX-100 for 10 minutes. Cells were blocked with 1% BSA/ 1X PBST (1X PBS +0.1% Tween 20) for 1 hr at RT. Cells were washed in 1X PBS, followed by incubation in primary antibody diluted in 1% BSA (in PBST) for

2hr at RT in humidified chamber. Coverslips were washed thrice in 1X PBS to remove excess primary antibody. Coverslips were incubated with secondary antibody diluted in 1% BSA (in PBST) for 1 hr at RT in a humidified chamber. Because of fluorescent tag on secondary antibody all samples were handled in dark from this step onwards. Secondary antibodies raised against two different species were mixed together in required concentrations and used. Coverslips were washed thrice with 1X PBS and stained with DAPI (0.5µg/µl in 2X FA/SSC) for 5 min at RT. Coverslips were washed thrice in 1X PBS, coverslips were mounted on glass slides using Slowfade Gold antifade and were sealed with DPX mountant.

Antibody information:

1. Rabbit anti Nup93- 1:500, sc-292099, Santa Cruz (Western blotting)
2. Rabbit anti CTCF- 1:500, Abcam (Western blotting blotting)
   1:500, 07-729, Millipore (ChIP)
3. Rabbit anti Nup188- 1:1000 Ab 86601,Abcam (Western)
4. Rabbit anti Nup205- 1:500 HPA024574, Atlas antibodies (Western blotting)
5. Mouse anti Oct4- 1:250, DHSB (Western blotting and IFA)
6. Donkey anti Rabbit IgG Horseradish peroxidase- 1:10,000, GE NA9340V
7. Sheep anti Mouse IgG HRP- 1:10,000, NA9310V

References

1. Andrews, P.W., Matin, M.M., Bahrami, A.R., Damjanov, I., Gokhale, P. and Draper, J.S. 2005. Embryonic stem (ES) cells and embryonal carcinoma (EC) cells: opposite sides of the same coin. *Biochemical Society Transactions* 33(Pt 6), pp. 1526–1530.
2. Buchwalter, A., Kaneshiro, J.M. and Hetzer, M.W. 2019. Coaching from the sidelines: the nuclear periphery in genome regulation. *Nature Reviews. Genetics* 20(1), pp. 39–50.
3. Capelson, M., Doucet, C. and Hetzer, M.W. 2010. Nuclear pore complexes: guardians of the nuclear genome. *Cold Spring Harbor Symposia on Quantitative Biology* 75, pp. 585–597.
4. Caricasole, A., Ward-van Oostwaard, D., Zeinstra, L., van den Eijnden-van Raaij, A. and Mummery, C. 2000. Bone morphogenetic proteins (BMPs) induce epithelial differentiation of NT2D1 human embryonal carcinoma cells. *The International Journal of Developmental Biology* 44(5), pp. 443–450.
5. D'Angelo, M.A., Gomez-Cavazos, J.S., Mei, A., Lackner, D.H. and Hetzer, M.W. 2012. A change in nuclear pore complex composition regulates cell differentiation. *Developmental Cell* 22(2), pp. 446–458.
6. Ibarra, A., Benner, C., Tyagi, S., Cool, J. and Hetzer, M.W. 2016. Nucleoporin-mediated regulation of cell identity genes. *Genes & Development* 30(20), pp. 2253–2258.
7. Ishihara, K., Nakamoto, M. and Nakao, M. 2016. DNA methylation-independent removable insulator controls chromatin remodeling at the HOXA locus via retinoic acid signaling. *Human Molecular Genetics* 25(24), pp. 5383–5394.
8. Jeudy, S. and Schwartz, T.U. 2007. Crystal structure of nucleoporin Nic96 reveals a novel, intricate helical domain architecture. *The Journal of Biological Chemistry* 282(48), pp. 34904–34912.
9. Kelly, G.M. and Gatie, M.I. 2017. Mechanisms regulating stemness and differentiation in embryonal carcinoma cells. *Stem cells international* 2017, p. 3684178.
10. Kurosawa, H. 2007. Methods for inducing embryoid body formation: in vitro differentiation system of embryonic stem cells. *Journal of Bioscience and Bioengineering* 103(5), pp. 389–398.
11. Labade, A.S., Karmodiya, K. and Sengupta, K. 2016. HOXA repression is mediated by nucleoporin Nup93 assisted by its interactors Nup188 and Nup205. *Epigenetics & Chromatin* 9, p. 54.
12. Mallo, M., Wellik, D.M. and Deschamps, J. 2010. Hox genes and regional patterning of the vertebrate body plan. *Developmental Biology* 344(1), pp. 7–15.
13. Narendra, V., Rocha, P.P., An, D., Raviram, R., Skok, J.A., Mazzoni, E.O. and Reinberg, D. 2015. CTCF establishes discrete functional chromatin domains at

the Hox clusters during differentiation. *Science* 347(6225), pp. 1017–1021.
14. Pascual-Garcia, P. and Capelson, M. 2014. Nuclear pores as versatile platforms for gene regulation. *Current Opinion in Genetics & Development* 25, pp. 110–117.
15. Pascual-Garcia, P., Jeong, J. and Capelson, M. 2014. Nucleoporin Nup98 associates with Trx/MLL and NSL histone-modifying complexes and regulates Hox gene expression. *Cell reports* 9(2), pp. 433–442.
16. Raices, M., Bukata, L., Sakuma, S., Borlido, J., Hernandez, L.S., Hart, D.O. and D'Angelo, M.A. 2017. Nuclear pores regulate muscle development and maintenance by assembling a localized mef2c complex. *Developmental Cell* 41(5), p. 540–554.e7.
17. Raices, M. and D'Angelo, M.A. 2012. Nuclear pore complex composition: a new regulator of tissue-specific and developmental functions. *Nature Reviews. Molecular Cell Biology* 13(11), pp. 687–699.
18. Robson, M.I., de Las Heras, J.I., Czapiewski, R., Lê Thành, P., Booth, D.G., Kelly, D.A., Webb, S., Kerr, A.R.W. and Schirmer, E.C. 2016. Tissue-Specific Gene Repositioning by Muscle Nuclear Membrane Proteins Enhances Repression of Critical Developmental Genes during Myogenesis. *Molecular Cell* 62(6), pp. 834–847.
19. Rousseau, M., Crutchley, J.L., Miura, H., Suderman, M., Blanchette, M. and Dostie, J. 2014. Hox in motion: tracking HoxA cluster conformation during differentiation. *Nucleic Acids Research* 42(3), pp. 1524–1540.
20. Toyama, B.H., Savas, J.N., Park, S.K., Harris, M.S., Ingolia, N.T., Yates, J.R. and Hetzer, M.W. 2013. Identification of long-lived proteins reveals exceptional stability of essential cellular structures. *Cell* 154(5), pp. 971–982.
21. Xu, M., Zhao, G.-N., Lv, X., Liu, G., Wang, L.Y., Hao, D.-L., Wang, J., Liu, D.-P. and Liang, C.-C. 2014. CTCF controls HOXA cluster silencing and mediates PRC2-repressive higher-order chromatin structure in NT2/D1 cells. *Molecular and Cellular Biology* 34(20), pp. 3867–3879.
22. Zhang, X., Huang, C.T., Chen, J., Pankratz, M.T., Xi, J., Li, J., Yang, Y., Lavaute, T.M., Li, X.-J., Ayala, M., Bondarenko, G.I., Du, Z.-W., Jin, Y., Golos, T.G. and Zhang, S.-C. 2010. Pax6 is a human neuroectoderm cell fate determinant. *Cell Stem Cell* 7(1), pp. 90–100.